MEASUREMENTS OF ELECTRON NUMBER DENSITY FLUCTUATIONS NEAR THE PLASMAPAUSE FROM THE CRRES SPACECRAFT

by

Michael Joseph LeDocq

A thesis submitted in partial fulfillment of the
requirements for the Master of Science degree in
Physics in the Graduate College of
The University of Iowa

August 1993

Thesis supervisor: Professor Donald A. Gurnett

Graduate College
The University of Iowa
Iowa City, Iowa

CERTIFICATE OF APPROVAL

MASTER'S THESIS

This is to certify that the Master's thesis of

Michael Joseph LeDocq

has been approved by the Examining Committee for the thesis requirement for the Master of Science degree in Physics at the August 1993 graduation.

Thesis committee: Thesis supervisor

Member

Member

Member

ACKNOWLEDGEMENTS

This project was completed with the help of many people who deserve my thanks. First and foremost, I would like to express my sincere gratitude to my adviser, Professor Donald Gurnett, who provided the initial concept for this project. Completion of this project would not have been possible without his many hours of patient instruction and guidance. I would also like to thank Dr. Roger Anderson, who provided many useful discussions. His knowledge of the CRRES spacecraft and Plasma Wave Experiment were of inestimable value. I would also like to extend my thanks to Mark Brown and Troy Shehan who traced most of the spectrograms and to Bob Lane and other plasma wave group programmers who assisted with much of the computer programming included in this work. My thanks also go to Jean Hospodarsky, Kathy Kurth, Bill Martin, and Michelle Govostes who helped type and format this paper; and to Joyce Chrisinger who drafted several of the illustrations.

The understanding and encouragement of many friends was invaluable and often helped me to retain my perspective and sanity while I worked. Anthony Minter, Fred Olchowski, David Dunn, Julia Andersen, Paul Foth, and my other fellow graduate students in the Physics Department deserve my thanks for living and working with me and for providing many helpful conversations. My special thanks are given to all of my friends at the Newman Catholic Student Center, especially the Bobs, whose emotional and spiritual support were always more than I could ever have asked for.

emotional and spiritual support were always more than I could ever have asked for. Most importantly I thank my family; especially my mother and father, my sister, Cherie, and my brother, Greg. They have been constant sources of support and encouragement and have always enhanced my successes.

This research was supported by contract 9-X29-D9711-1 with Los Alamos National Laboratory; contract F19628-90K0031 with the United States Air Force, Hanscom Air Force Base; and funds from the University of Iowa Graduate College.

ABSTRACT

Large quasiperiodic fluctuations in the electron number density are often encountered near the plasmapause and in the plasmasphere by the CRRES satellite. The sweep frequency receiver in the CRRES Plasma Wave Experiment gives high-frequency-resolution measurements of these density fluctuations by providing one electric field spectrum every eight seconds in the frequency range 6.4 kHz to 400 kHz. Electron number density values are calculated from emissions at the upper hybrid resonance frequency and from cutoffs at the electron plasma frequency. A power spectral analysis reveals electron density fluctuations with frequencies ranging from 2 mHz to approximately 61 mHz, the highest density fluctuation frequency that can be resolved by this analysis. Quasiperiodic fluctuations have been found outside the plasmasphere with spatial scales along the orbit path of approximately 750 km. Plasma density irregularities in the outer plasmasphere sometimes have power spectral slopes near $-5/3$ which suggests the presence of well-developed two-dimensional magnetohydrodynamic turbulence. The large quantity of electron density values provided by CRRES during its 15 month lifetime also allows a statistical analysis to be performed. The root-mean-square value of the electron density fluctuation amplitude normalized by the average local electron density, $(n_e)_{rms}/\langle n_e \rangle$, has been calculated for 5.5 minute intervals from August through December 1990. The largest density

fluctuation amplitudes occur between L = 3 and L = 6, the region in which the plasmapause is located. The density fluctuation amplitudes decrease with increasing L-shell for L > 6. Normalized fluctuation amplitudes greater than 10% are found in only 25% of the available data of this study. A complete study of fluctuation amplitude with respect to local time is not possible until density values from 1991 CRRES orbits become available. A preliminary study did not show a significant local time dependence.

TABLE OF CONTENTS

LIST OF FIGURES

CHAPTER I. INTRODUCTION

The objective of this thesis is to study small scale plasma density fluctuations using plasma wave observations from the Combined Release and Radiation Effects Satellite (CRRES). This spacecraft provides measurements near the equatorial plane at radial distances extending out to about 6.3 R_E (Earth radii). Several previous spacecraft, most notably OGO 5, GEOS 1 and GEOS 2, have provided plasma density measurements in this same region. The plasma density measurements made by the light ion mass spectrometer on OGO 5 had a time resolution of 4 seconds (Harris and Sharp, 1969). The OGO 5 data showed large density fluctuations near the plasmapause in the bulge region after periods of enhanced fluctuating geomagnetic activity (Chappell et al., 1970; Carpenter and Chappell, 1973). The relaxation sounder experiments onboard GEOS 1 and GEOS 2 produced electron density measurements once every 22 seconds in the routine operating mode, or once every 86 ms in the f_{pe} tracking mode (Higel, 1978; Higel and Lei, 1984). The GEOS 1 data showed density fluctuations with periods of 3 to 4 minutes at some plasmapause crossings. GEOS 1 also observed fluctuations with amplitudes of 1 to 3% and periods of approximately 10 seconds in other regions of the magnetosphere (Higel, 1978), although no in-depth study of density fluctuations was undertaken.

Other types of density structures also occur near the plasmapause. Longitudinal ripples in the dayside plasmapause with peak to peak amplitudes of up to 0.4 R_E were identified in early whistler studies of the plasmapause (Carpenter, 1966; Angerami and Carpenter, 1966; Park and Carpenter, 1970) and ripple-like plasma density structures were also encountered by the OGO 5 satellite (Chappell, 1972). Chappell (1972) proposed that structures of this type could be detached plasma regions that peel off from the plasmasphere on the dayside and eventually corotate to the evening-dusk sector. Other studies of the OGO 5 data (Chappell et al., 1971; Chappell, 1974) have found these detached regions to be located most often in the afternoon-dusk sector and less often in the dayside sector. Similar structures were also observed by the S^3-A satellite (Maynard and Cauffman, 1973). Further studies have interpreted similar density structures as plasmatails that are formed in the bulge region and then wrap longitudinally around the main plasmapause (Chen and Wolf, 1972). Models using various electric field configurations have had some success in producing behavior resembling the characteristics of detached plasma regions and small scale density irregularities detected by whistlers and satellite-born experiments (Chen and Wolf, 1972; Chen and Grebowsky, 1974; Grebowsky and Chen, 1976).

Small scale quasiperiodic fluctuations in electron number density are often observed near the plasmapause by the plasma wave instrument on the CRRES spacecraft. The high resolution density data provided by the CRRES plasma wave instrument make it possible to study the characteristics of density irregularities with

amplitudes and scale lengths that are small compared to the plasmapause. Also, the large size of the data set makes a statistical analysis of the location of the density irregularities possible.

CHAPTER II. CRRES SPACECRAFT AND DATA HANDLING

The plasmasphere is a toroidal region of dense plasma near the Earth and is shown in a noon-midnight meridional cross section of the Earth's magnetosphere in Figure 1 (Chappell, 1972). Figure 2 is an L-local time plot of the plasmasphere determined by more than 150 passes of the OGO 5 spacecraft (Chappell et al., 1971). The plasmapause is the outer boundary of the plasmasphere and is observed as a sharp decrease in plasma density between the high-density plasmasphere and the low-density plasma of the magnetosphere outside the plasmasphere. The CRRES spacecraft remains in or near the plasmasphere during its entire orbit, and provides high time resolution electron number density data near the plasmapause twice per orbit. This section of the paper describes the CRRES orbit, the plasma wave instrumentation, and the procedures used to produce electron density values.

CRRES Orbit Parameters and Plasma Wave Instrument

The CRRES spacecraft was launched on July 25, 1990 (Anderson et al., 1992) into an elliptical Earth orbit with an initial perigee of 350 km and an apogee of 6.3 R_E (Earth radii) geocentric. The orbit has an inclination of 18.2 degrees, a period of 9 hours 52 minutes and an initial magnetic local time at apogee of 0800.

The CRRES Plasma Wave Experiment includes a spectrum analyzer that produces high-time-resolution electric field spectra in the frequency range from 5 Hz to 10 MHz and a sweep frequency receiver that produces high-frequency-resolution electric field spectra in the frequency range from 100 Hz to 400 kHz. The sweep frequency receiver measurements are obtained in four frequency bands with 32 steps per band. Band 1 (100 to 800 Hz) produces one spectrum per 32 seconds. Band 2 (800 Hz to 6.4 kHz) produces one spectrum per 16 seconds. Band 3 (6.4 kHz to 50 kHz) and Band 4 (50 kHz to 400 kHz) are each sampled at a rate of 4 steps/s, and produce one spectrum every 8 seconds. The electron number density is calculated from narrowband emissions at the upper hybrid resonance frequency, f_{UHR}, and from the cutoff at the plasma frequency, f_p, of continuum radiation. Because these emissions usually occur in bands 3 and 4, electron number density values are normally produced every 8 seconds. This sampling rate is higher than that produced by previous spacecraft and allows the study of density fluctuations with periods as small as 16 seconds. Figure 3 shows a spectrogram produced by the CRRES plasma wave experiment during an inbound plasmapause crossing on September 15, 1990 from 02:17:59 UT to 04:07:04 UT. Universal Time is plotted along the horizontal axis. The horizontal scale also provides the spacecraft coordinates such as the geocentric radial distance in units of Earth radii (R_E), the McIlwain L-parameter, and the magnetic local time (MLT) in hours. The highest intensity emissions are represented by red and the lowest intensity emissions are represented by dark blue. Frequencies from 5 Hz to

400 kHz are plotted logarithmically on the vertical scale. The 5 Hz to 100 Hz portion of the spectrogram is derived from the spectrum analyzer and the 100 Hz to 400 kHz portion is produced by the sweep frequency receiver. The electron cyclotron frequency, which is proportional to the magnetic field strength, is plotted as the white curve across the spectrogram.

Computation of the Electron Number Density

Narrowband upper hybrid resonance emissions are often detected in the plasmasphere, and often make a smooth transition to a cutoff of continuum radiation emissions at the electron plasma frequency outside the plasmapause (Shaw and Gurnett, 1975). These emissions are frequently observed in the CRRES spectrograms and provide a useful method of calculating the electron number density. The plasma frequency cutoff of continuum radiation is present from approximately 02:18 UT to 02:40 UT in the upper portion of the spectrogram in Figure 3. The cutoff frequency makes a smooth transition to emissions at the upper hybrid resonance frequency at approximately 02:40 UT. A computer program allows these emissions to be traced by hand. To trace the emissions the spectrogram is displayed on the computer screen in an expanded format and a mouse and pointer are used to digitize the frequency of upper hybrid emissions inside the plasmapause and cutoffs at the electron plasma frequency outside the plasmapause. The computer program used to digitize the spectrogram information also calculates the electron number density.

The electron plasma frequency is given by

$$f_p = \frac{1}{2\pi} \left[\frac{n_e e^2}{\epsilon_0 m_e}\right]^{\frac{1}{2}} \quad , \text{ or} \tag{1a}$$

$$f_p \simeq 8.98 \sqrt{n_e} \text{ kHz} \tag{1b}$$

where n_e is the electron number density, e is the electron charge, m_e is the electron mass, and ϵ_0 is the permittivity of free space. Equation (1b) gives the plasma frequency in kHz when the electron number density is given in electrons/cm^3. The upper hybrid resonance frequency is given by

$$f_{UHR} = (f_{ce}^2 + f_p^2)^{\frac{1}{2}} \tag{2}$$

where the electron cyclotron frequency, f_{ce}, is given by

$$f_{ce} = \frac{e B}{2\pi m_e} \quad , \text{ or} \tag{3a}$$

$$f_{ce} \simeq 2.8 \times 10^6 \text{ B Hz} \tag{3b}$$

where B is the magnetic field strength. The units of f_{ce} in equation (3b) are Hz when the magnetic field strength has units of Gauss. The electron number density is calculated directly from equations (1b) or (2). When the plasma frequency has been traced, the electron number density is calculated using the relation

$$n_e = \left(\frac{f_p}{8.98}\right)^2 \tag{4}$$

where f_p is in kHz. When the upper hybrid resonance frequency is provided, the number density is calculated using

$$n_e = \frac{f_{UHR}^2 - f_{ce}^2}{(8.98)^2} \tag{5}$$

where f_{UHR} and f_{ce} are in kHz. Once the spectrograms have been traced the resulting electron number density data files can then be analyzed using procedures that will be discussed in chapters III and IV.

Error Analysis of Tracing Procedure

Upper hybrid and plasma frequency emissions are often detected in several frequency channels during a given 8.192 second sweep interval. This spread in frequency introduces errors in the tracing procedure. In many cases it is appropriate to choose the pixel which represents the frequency channel which contains the most

intense emission. Where continuum radiation is clearly present it is usually appropriate to choose the frequency at which the cutoff of the emissions occur. Sometimes cases occur where there is no clear indication of the correct choice of frequency channel. It is therefore necessary to calculate the error introduced by individual interpretation of the tracing procedure and to compare this error with the amplitude of the density fluctuations that are being studied.

The spectral analysis, described in the next chapter, examines the power spectra of selected density profiles. These spectra are produced by performing a fast Fourier transform on the density time series and plotting the squares of the Fourier coefficients versus frequency. The spectrum of the difference of two traces of the same time period can be used to evaluate the error spectrum introduced by the tracing procedure. The difference of the data from two separate tracings of the same time period is calculated. The power spectrum of the difference of the two traces is the error spectrum for this time series. Interpretation of the power spectrum is reliable only where the level of the power spectrum is greater than the level of the error spectrum. The power spectra and error spectra included in this analysis have amplitudes that are comparable for frequencies greater than 0.03 to 0.04 Hz. Therefore, conclusions are based on spectral components with frequencies less than 0.03 to 0.04 Hz.

CHAPTER III. SPECTRAL ANALYSIS OF DENSITY FLUCTUATIONS

Analysis Procedure

Electron density profiles are plotted using the values calculated from the tracing program. For example, the density profile produced by tracing the upper hybrid emission from the spectrogram in Figure 3 is plotted as the upper line in Figure 4. This line gives the density profile from 02:47:28 UT to 03:15:44 UT on September 15, 1990 immediately following the inbound plasmapause crossing of orbit 124. In order to analyze only the small-scale fluctuations, the longest period density fluctuations are removed from the density time series by using a detrending process. Fluctuations with periods of 500 seconds or longer are removed by using an averaging period of sixty-one data points that corresponds to approximately 500 seconds in the time series. The arithmetic mean of the first sixty-one data points is subtracted from the thirtieth point to produce the first detrended point. Next, the mean of the second through the sixty-second points is subtracted from the thirty-first data point to produce the second detrended point. The same process is used with the third through the sixty-third data points and is continued to the end of the time series being analyzed. The values produced by using this "sliding average" of the original time series are interpreted as a measure of the large scale behavior of the density profile. Subtracting the sliding average values from the original density profile yields a detrended time series with the

characteristics of the small scale fluctuations, as shown in Figure 5. The detrending process using a time period of 500 seconds acts as a low-pass filter which removes fluctuations with periods of 500 seconds or greater. The corresponding frequency is approximately 2 mHz and frequencies lower than this value are filtered out as a result of the detrending process. These detrended data are plotted as the lower line in each of the time series plots and fluctuate about zero. The lower line in Figure 4 shows the density fluctuations corresponding to the density profile of 02:47:28 UT to 03:15:44 UT on September 15, 1990. A peak is present at 2 mHz in all of the power spectra as a result of this detrending process and is ignored unless density structures with periods of about 500 seconds are clearly present in the time series.

To compute the power spectrum of the density fluctuations a fast Fourier transform is then performed on each density profile. The power spectrum is given by the squares of the FFT coefficients for the profile being analyzed. A linear plot of the power spectrum is useful for identifying any characteristic frequencies that might be present in the observed density fluctuations. The maximum frequency plotted is 61.04 mHz, which is the Nyquist frequency corresponding to the SFR sampling rate of 8.192 seconds. The power spectrum can also be plotted on a log-log scale to test for the presence of well-developed, two-dimensional magnetohydrodynamic (MHD) turbulence. The power spectrum of two-dimensional turbulence is expected to be the Kolmogorov spectrum, $P \propto k^{-5/3}$ (Biskamp and Welter, 1989), where P is the power represented by the FFT coefficients squared, and k is the wave number. The spacecraft is assumed

to be moving through stationary density structures so that the wave number is proportional to the frequency. The slope of the log-log plot should then have a slope of $-5/3$ if a Kolmogorov spectrum is present.

As the first step in the analysis the power spectra are computed directly from the FFT coefficients, with no spectral smoothing or averaging. All details of the original spectrum are shown, and a line with a slope of $-5/3$ is drawn for comparison to the Kolmogorov spectrum. Spectral smoothing is used to increase the statistical reliability of each component of the power spectrum. Spectral smoothing is accomplished by convolving the original power spectrum with a filter function of a specified shape and width (Sentman, 1974). The power spectra in this analysis have been smoothed with a Gaussian filter of width 0.01 Hz. The statistical reliability of the individual spectral components is increased and the general trend of the power spectra is shown. The 80% confidence factor is shown in each spectrum for a typical spectral point. The FORTRAN program PWRFFT written by A. Fey is used to calculate the power spectra, to perform spectral smoothing and to provide error bars (Spangler et al., 1988).

Experimental Results

The power spectral analysis was carried out for several time periods that exhibit clear density fluctuations. The time periods below are labeled by the date and starting time of the spectrogram from which the density profile is traced.

September 15, 1990, 02:38 UT

Figure 4 shows the density profile from the inbound pass of orbit 124 from 02:47:28 to 03:15:44 UT on September 15, 1990. The spacecraft crosses the plasmapause near 02:31 UT and is in the plasmasphere for the duration of this time series. The density fluctuations seem to be random, with no obviously sinusoidal behavior. The unfiltered power spectrum for this time period is shown as the top curve in Figure 6. This spectrum has a spectral resolution of 0.00082 Hz. The lower curve is the error spectrum for this time period. The level of the error spectrum approaches the level of the power spectrum at frequencies greater than 30 to 40 mHz. The power spectrum appears to have a slope that is similar to the Kolmogorov spectrum for frequencies less than 40 mHz. Figure 7 shows the power spectrum after smoothing with a Gaussian filter of width 0.01 Hz. This results in a spectral resolution of 0.01 Hz. The spectrum has a slope which is slightly more negative than the Kolmogorov spectrum.

September 20, 1990, 20:26 UT

The density profile in Figure 8 shows data obtained form 21:01:32 UT to 21:28:59 UT on September 20, 1990 during the inbound portion of orbit 138. Density fluctuation amplitudes of approximately 200 cm^{-3} are present during the entire time series. The power spectrum shown by the upper curve in Figure 9 has a slope which is very nearly $-5/3$. This spectrum has a spectral resolution of 0.00086 Hz. The error

spectrum, shown by the lower curve in Figure 9, is very close to the level of the power spectrum at frequencies greater than 0.03 Hz. The smoothed spectrum shown in Figure 10 has a spectral resolution of 0.01 Hz. The slope is again very nearly $-5/3$, so it is likely that 2-D MHD turbulence may be occurring during this time series.

September 4, 1990, 13:59 UT

The density profile from 14:07:29 UT to 14:35:28 UT during the outbound portion of orbit 99 is shown in Figure 11. The spacecraft is in the outer plasmasphere and crosses the plasmapause near 14:35 UT. The density fluctuations have a maximum amplitude of approximately 30 cm^{-3}. The power spectrum is shown as the upper curve in Figure 12. The error spectrum again appears to have amplitudes comparable to the level of the power spectrum for frequencies above 0.04 Hz. The slope of this spectrum is also similar to the Kolmogorov spectrum. Figure 13 shows the filtered power spectrum and error spectrum for this time series. The spectral resolution is 0.01 Hz. This spectrum also has a slope that is near $-5/3$ indicating that 2-D MHD turbulence may be present during this time.

November 6, 1990, 01:52 UT

The density profile produced on November 6, 1990 from 01:52:28 UT to 03:41:33 UT during the outbound pass of orbit 251, shown in Figure 14, differs from the previous examples in that the electron density stays relatively constant with a lower

average density throughout the entire time period while still containing significant density fluctuations. The spacecraft is outside the plasmasphere during this entire time series. The power spectrum of this time series showed one large peak near 0.002 Hz when a period of 500 seconds was used in the detrending process. To determine if a spectral component not due to the detrending process is present at 0.002 Hz, this time series was detrended using a 1500 second time period. The 1500 seconds detrending period produces the peak near 0.0007 Hz in the power spectrum shown in Figure 15. A peak is still present at 0.0024 Hz although the error of a spectral component is greater than the amplitude of the peak. Figure 16 shows the smoothed spectrum with a spectral resolution of 0.001 Hz. A peak is still present during this time. The average satellite velocity, v_s, can be used to approximate the spatial size of density irregularities with these frequencies. The average spacecraft velocity for this time period is 1.81 km/s. The wavelengths for irregularities with this frequency is found by using

$$\lambda = \frac{v_s}{f} \tag{6}$$

Fluctuations with a frequency of 0.0024 Hz will then have a wavelength of approximately 750 km along the spacecraft orbit.

CHAPTER IV. STATISTICAL ANALYSIS

The purpose of this statistical analysis is to determine the correlation of the amplitude of the electron density fluctuations with various magnetospheric coordinates such as the McIlwain L-parameter and magnetic local time. The electron density data analyzed includes all available density data from August 1, 1990 when the sweep frequency receiver was switched on, to December 22, 1990, when the SFR was switched off for several weeks. Traces after this time have not been completed and restrict analysis of local time dependence, as will be discussed later in this chapter.

Analysis Procedure

The normalized amplitude of density fluctuations is calculated for a time period approximately 5.5 minutes long. This length of time was chosen so that the change in L-shell along the orbit remains less than 0.5. The maximum change in L-shell for this period of time is approximately 0.3. The normalized density fluctuation amplitude is calculated by first finding the standard deviation, σ, of the density values in the first 5.5 minute time interval. The sample standard deviation is given by:

$$\sigma = =[\frac{\sum (x_i - \langle x \rangle)^2}{n-1}]^{\frac{1}{2}} \qquad (7a)$$

or, for use in a computer algorithm,

$$\sigma = \left[\frac{\sum x_i^2 - (\sum x_i)^2}{n(n-1)}\right]^{\frac{1}{2}} \qquad (7b)$$

and is approximately equal to the root-mean-square average of the density fluctuations during the interval. The individual data points are denoted by x_i, the average of the data points on the interval is $\langle x \rangle$, and n is the number of data points included during the interval. The standard deviation is then divided by the average density of the time interval. This quantity, $\sigma/\langle x \rangle$, is called the coefficient of variation and gives the approximate rms density fluctuation amplitude as a percentage of the average density during the time interval. The coefficient of variation for the electron number density is denoted by $(n_e)_{rms}/\langle n_e \rangle$ on Figures 17 through 23. Subsequent 5.5 minute time intervals have 50% overlap. This overlapping is performed to ensure continuous coverage of the data to reduce information loss in the analysis without oversampling the original data. Calculation of the coefficient of variation for these overlapping time intervals continues until the end of the data file. This analysis is then performed on other available data files and the results are collected in one output file.

Results of the Statistical Analysis

The normalized density fluctuation amplitudes calculated for the data from August 1, 1990 through December 22, 1990 are plotted versus L-shell. The scatter plot

of these data are shown in Figure 17. The density irregularity amplitudes range from zero percent (no fluctuation) to almost 200% of the average density during a 5.5 minute time interval. Density irregularities of greater than 100% of the average occur in this analysis when the standard deviation is calculated for a series of data containing a steep gradient. If large fluctuations in the data occur while there is a steep gradient in the data over the interval being observed, a standard deviation greater than the average can be obtained. Density fluctuation amplitudes greater than 100% probably occur during the steep density gradients which can be encountered during distinct plasmapause crossings, detached plasma region crossings, or satellite encounters with other density structures.

Figure 17 also shows that the largest fluctuation amplitudes occur for L values between 3 and 6. This result suggests that the largest density irregularities are probably associated with the plasmapause. The maximum density fluctuation amplitudes decrease for L-shell values greater than 5, i.e. the density fluctuation amplitude decreases with increasing L-shell. Figures 18 and 19 show the same data plotted as quartiles on linear scale and on a logarithmic scale with bins 0.5 L in width from L=1 to L=8.5. Figure 18 clearly shows that the maximum density fluctuation amplitude occurs in the $3.5 < L < 4.0$ bin and that the maximum decreases for $L > 4.0$, with the exception of the $6.0 < L < 7.0$ bins. The event which corresponds to this large amplitude fluctuation will be discussed later in this section. The 25th, 50th, and 75th percentiles all occur at values much less than the maximum value of the data. The log scale of

Figure 19 shows clearly that for most of the L-shell ranges the 25th and 50th percentiles of the fluctuations measured have amplitudes less than 10% of the average number density. For $L > 5.5$ the 25th percentile contains fluctuations less than 1% of the average and for $6.5 < L < 8.0$ the 50th percentile also contains fluctuations less than 1% of the average. The 75th percentile contains fluctuation amplitudes between 10% and 20% of the average density until $L > 5.0$. For greater L values the amplitudes in the 75th percentile range between 5% and 10%. The 100th percentile for all L-shell ranges contain fluctuation amplitudes above 10% of the average density. This shows that no more than one quarter of the density data acquired from August through December 1990 contained density fluctuations with amplitudes greater than 10% of the average density. Outside the plasmapause the amplitude of the density fluctuations and the rate of occurrence of significant fluctuations clearly decreases with increasing L.

The large amplitude fluctuations which produce the spike at $L = 6.4$ in Figure 17 occur during two isolated time periods. A normalized density fluctuation amplitude of 1.18 is calculated from a 5.5 minute time period centered at 20:40:15 UT on October 3, 1990. At this time the spacecraft is at 5.01 hr magnetic local time (MLT), has a radial distance of 6.24 R_E, and an L-shell value of 6.39. Several other density fluctuation amplitudes greater than 1.0 are calculated from time intervals which range from 22:27:35 UT to 23:14:00 UT on October 5, 1990. Three of these occur during consecutive time periods from 22:27:35 UT to 22:33:02 UT during which the

satellite covers a local time range from 5.24 hr to 5.29 hr. The radial coordinates are $L = 6.41$ and $R = 6.26\ R_E$ for this time period and do not change appreciably because the satellite is at apogee. A fourth large fluctuation occurs at 22:57:37 UT with $L = 6.34$, MLT = 5.55 hr, and $R = 6.18\ R_E$. The fifth large fluctuation occurs at 23:14:00 UT with the spacecraft at $L = 6.27$, MLT = 5.72 hr and $R = 6.10\ R_E$. A comparison of these large fluctuations to magnetic activity measured by the D_{st} index showed no obvious correlation to magnetic storm or substorm activity. Further study is needed to determine the cause of the large density fluctuations for local times between $5.0 < \text{MLT} < 6.0$ and L-shell values between $6.0 < L < 6.5$.

A study of the dependence on local time of the number of density fluctuation occurrences and amplitudes of density fluctuations was attempted, but incomplete local time coverage of the traced spectrograms prevents reliable conclusions from being made. For the period of August to December 1990 the fluctuation amplitude values were plotted versus L-shell value for four magnetic local time sectors. The local time sectors 21.00 to 2.99 MLT and 3.00 to 8.99 MLT, Figures 20 and 21, contain most of the data shown in Figure 17. Both of these sectors exhibit the same trends found in the original data with the maximum density fluctuation amplitudes occurring between $L = 3$ to $L = 6$ and decreasing with increasing L for $L > 6$. The local time sector 9.00 to 14.99 MLT, Figure 22, has significantly fewer data points than the previous sectors and the 15.00 to 20.99 MLT sector, Figure 23, has only a small number of data values. This lack of density fluctuation amplitude calculations in some local time

sectors is due to incomplete local time coverage of the CRRES orbit between August and December 1990. When the spacecraft nears perigee and higher electron densities, the upper hybrid resonance frequency becomes higher than the 400 kHz frequency band of the SFR, and no f_{UHR} emissions can be detected until the satellite passes perigee and enters lower density regions on the outbound portion of the orbit. During the August to December 1990 period the orbit perigee advances from 19.91 MLT to 14.15 MLT. Spectrogram traces from CRRES orbits completed during 1991 are necessary to complete the local time coverage of the orbit and to conduct a valid study of local time dependence of density fluctuation amplitudes.

CHAPTER V. CONCLUSIONS

Small-scale electron density fluctuations are observed by the CRRES satellite in the magnetosphere near the plasmapause. Power spectral analysis of density profiles that contain data from the outer plasmasphere may have spectra that are similar to the Kolmogorov spectrum. Therefore, well-developed two-dimensional MHD turbulence apparently exists in these regions. In other cases, density profiles sometimes produce power spectra that contain distinct peaks, suggesting the presence of quasiperiodic fluctuations. Electron number densities in these time series range from about 1 cm^{-3} to 1000 cm^{-3}. The density fluctuations have amplitudes up to 200 cm^{-3}. The density fluctuations occur over a range of frequencies, from 2 mHz to almost 61 mHz. The upper limit of detectable density fluctuation frequencies is 61.04 mHz which corresponds to the smallest density fluctuation period of 16.384 seconds which is two times the sampling time interval of the upper frequency bands of the CRRES sweep frequency receiver.

The density fluctuations with the largest amplitudes occur between $L = 3$ and $L = 6$, the range in which the plasmapause is found. The density fluctuation amplitude decreases with increasing L for $L > 6$. During the period between August 1, 1990 and December 22, 1990 density fluctuation amplitudes of 10% or greater of the average local electron density were present in only 25% of the data collected. At least half of

the available density data contained fluctuations which were 1% or less of the average local density. In the magnetic local time sectors 21.00 to 2.99 MLT and 3.00 to 8.99 MLT the distribution of density fluctuation amplitude with respect to L-shell is similar to that observed in the full data set. Unfortunately, inadequate coverage of the remaining local time sectors makes a valid study of density fluctuation amplitude dependence on local time impossible.

Density structures in the plasmasphere have been studied recently using the Very Large Array radio-interferometer (Jacobson and Erickson, 1992). The density irregularities observed in this study are called magnetic-eastward-directed (MED) irregularities. Two cosmic radio sources are observed from each of two or three radio antenna pairs. These antenna pairs are located along an axis parallel to the line of motion of the observed density irregularities. The lines of sight of the antennas remain fixed on the radio sources which move westward across the sky as the Earth rotates. Density irregularities that are assumed to be located in the corotating plasmasphere will then appear to move eastward across the lines of sight of the antennas. Analysis of the motion of density irregularities across the lines of site to the radio sources are used to determine the trace-speed and altitude of these irregularities. These MED irregularities were originally thought to be located in the ionosphere, but recently the have been determined to occur in the plasmasphere and to corotate with the Earth. These irregularities occur most often in the L-shell range $2.0 \lesssim L \lesssim 3.0$. It was also found that the density irregularities in higher L-shells were observed at higher magnetic

latitudes. The irregularities have wavelengths perpendicular to the magnetic field of approximately 30 to 40 km and amplitudes on the order of 100 cm^{-3}. The results of the spectral analysis of the CRRES density data showed some density structures with spatial scales along the orbit of approximately 750 km. The electron density fluctuations occur in the L-shell range $1.5 < L < 8.5$. Although measurements are taken with magnetic latitude $\leq 18°$, and the scale length of the structures found in this spectral analysis are larger than the size of the MED irregularities found in the radio-interferometer study, some density structures observed in the CRRES density profiles may coincide with the size of the MED irregularities. This implies that some of the density structures observed by CRRES could be the same as the MED irregularities that are stationary with respect to, and corotating with, the plasmapause.

A study of possible mechanisms that produce these density irregularities is beyond the scope of this report, but a few possibilities can be mentioned. Park and Helliwell (1971) suggested that lightning discharges produce electric fields perpendicular to geomagnetic field lines. It is postulated that these electric fields are mapped into the plasmasphere along the field lines. The resulting **E** x **B** drift then causes flux tubes to rotate about the magnetic field lines. Flux tubes with smaller electron density rotate inward and are replaced by higher density tubes that are rotating outward. This interchange appears as a fluctuation in a density profile produced by a spacecraft flying through such a structure. Density irregularities could also be produced by MHD waves or plasma depletions in flux tubes caused by ionospheric effects.

Finally, two-dimensional MHD turbulence could be caused by a velocity shear at the plasmapause. The plasma inside the plasmapause corotates with the Earth and flows with a velocity relative to the non-rotating plasma outside the plasmapause. This velocity shear will produce a Kelvin-Helmholtz instability at the plasmapause that can evolve into well developed turbulence.

Figure 1. A noon-midnight meridional cross section of the Earth's magnetosphere, showing the plasmasphere. (Figure reproduced from Chappell (1972)).

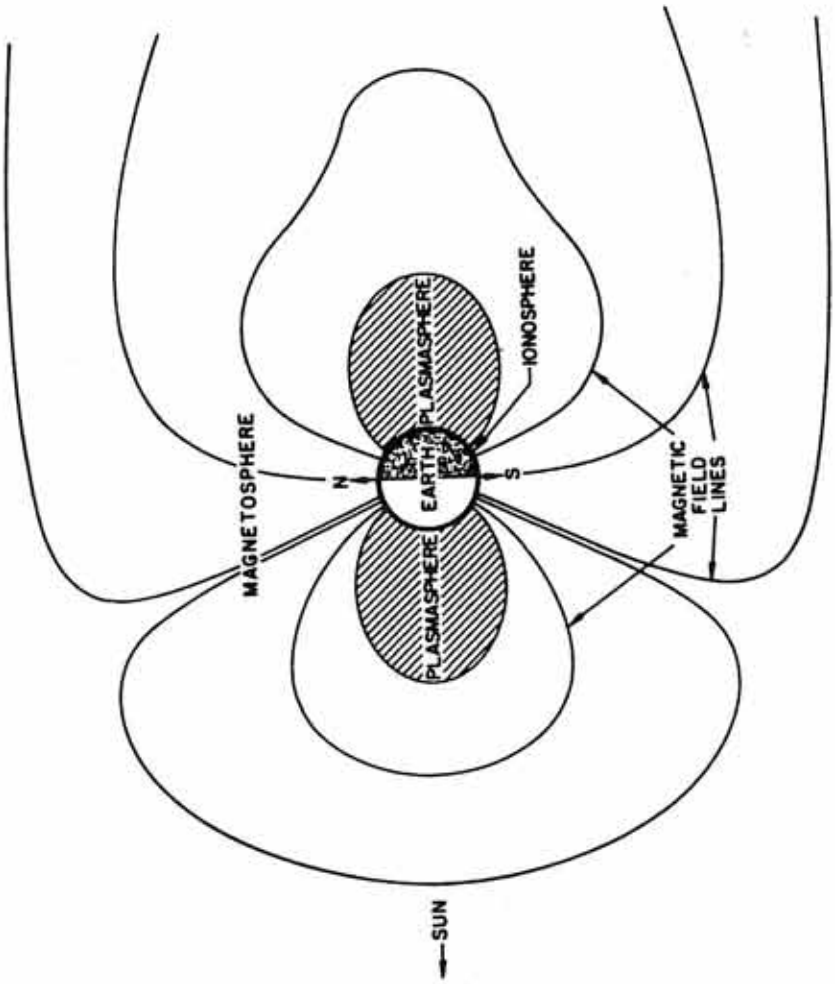
MAGNETOSPHERE
N
PLASMASPHERE
IONOSPHERE
EARTH
S
MAGNETIC FIELD LINES
PLASMASPHERE
SUN

Figure 2. An L-local time plot of the plasmasphere determined from OGO 5 data. (Figure reproduced from Chappell et al. (1971)).

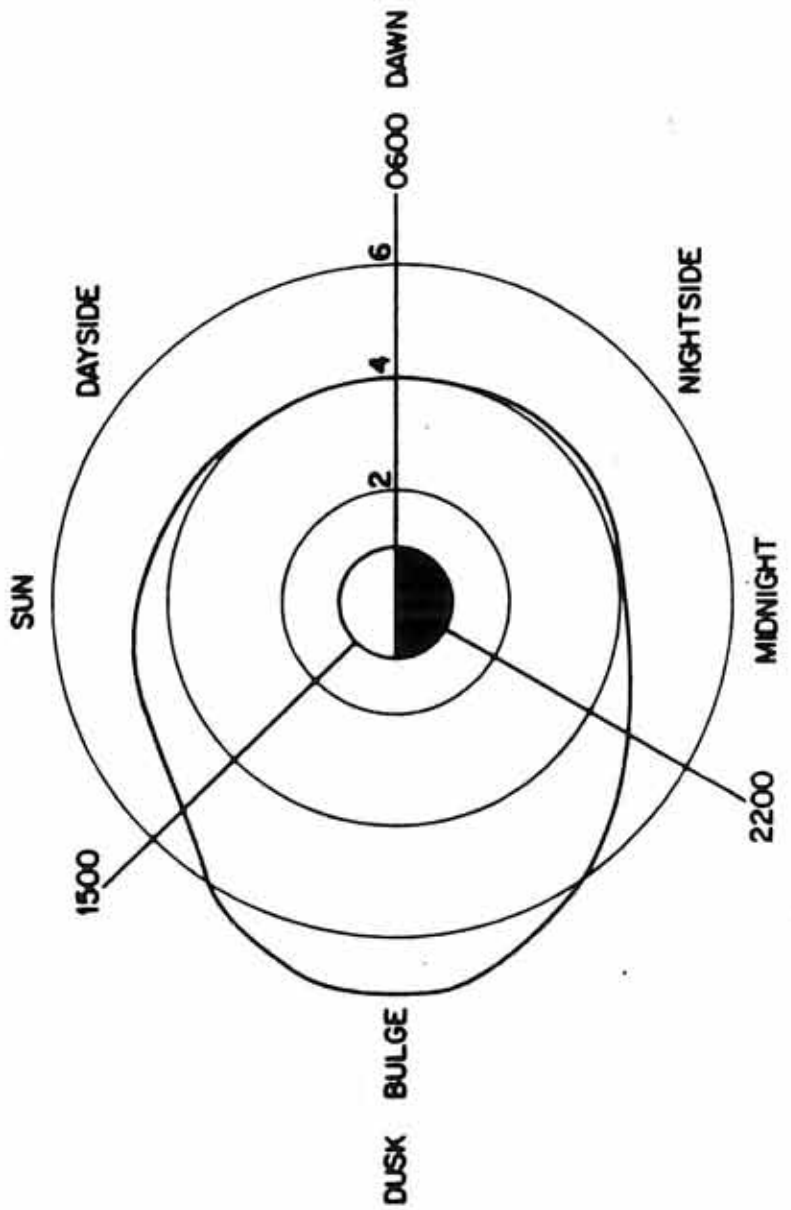
DAWN
0600
6
4
2
DAYSIDE
NIGHTSIDE
SUN
MIDNIGHT
1500
2200
DUSK BULGE

Figure 3. A frequency-time spectrogram of data from the CRRES Plasma Wave Experiment sweep frequency receiver for the time interval from 02:17:59 UT to 04:07:04 UT, September 15, 1990 during the inbound portion of orbit 124. The cutoff of continuum radiation at the plasma frequency and the narrow band emission at the upper hybrid frequency are clearly shown.

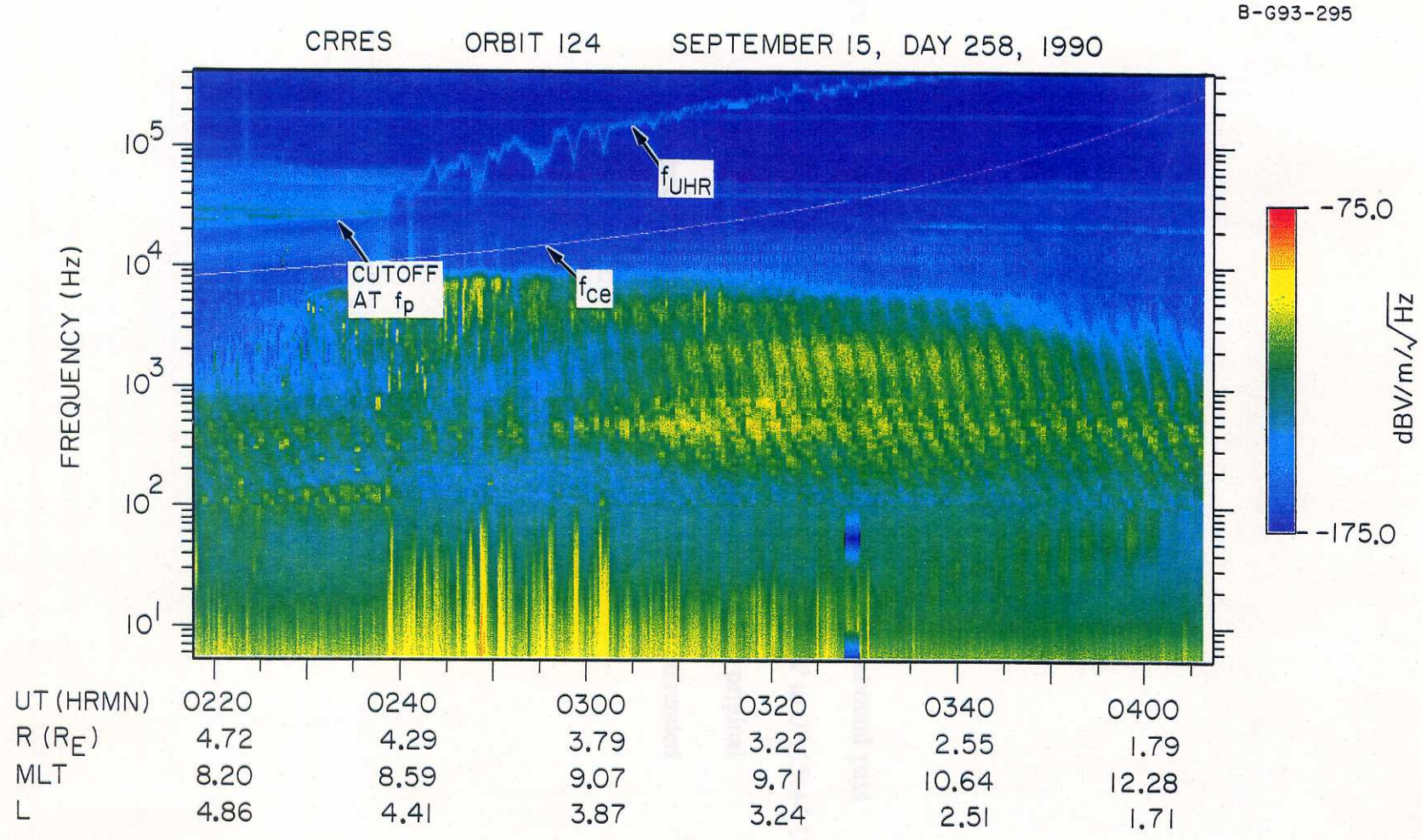
B-G93-295
CRRES ORBIT 124 SEPTEMBER 15, DAY 258, 1990
FREQUENCY (Hz)
10^5
10^4
10^3
10^2
10^1
f_{UHR}
CUTOFF AT f_p
f_{ce}
-75.0
-175.0
dBV/m/√Hz
UT (HRMN) 0220 0240 0300 0320 0340 0400
R (R_E) 4.72 4.29 3.79 3.22 2.55 1.79
MLT 8.20 8.59 9.07 9.71 10.64 12.28
L 4.86 4.41 3.87 3.24 2.51 1.71

Figure 4. Electron number density time series during the inbound pass of orbit 124. Data are shown from 02:47:28 UT to 03:15:44 UT on September 15, 1990. The upper curve is the original electron density profile, the lower curve is the detrended density profile.

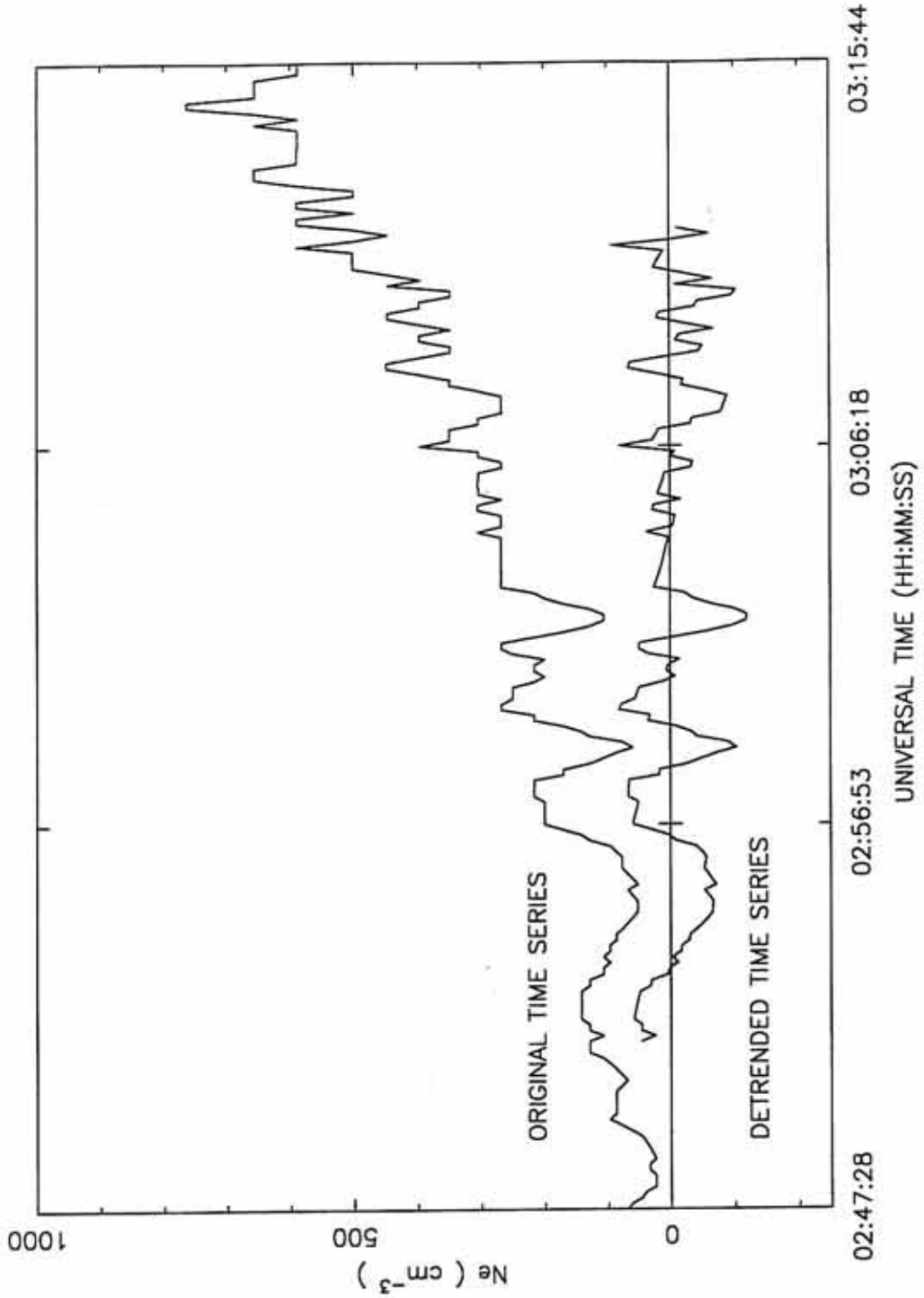
1000
500
0
Ne (cm^{-3})
ORIGINAL TIME SERIES
DETRENDED TIME SERIES
02:47:28
02:56:53
03:06:18
03:15:44
UNIVERSAL TIME (HH:MM:SS)

Figure 5. Generalized density profile illustrating the steps in the detrending process.

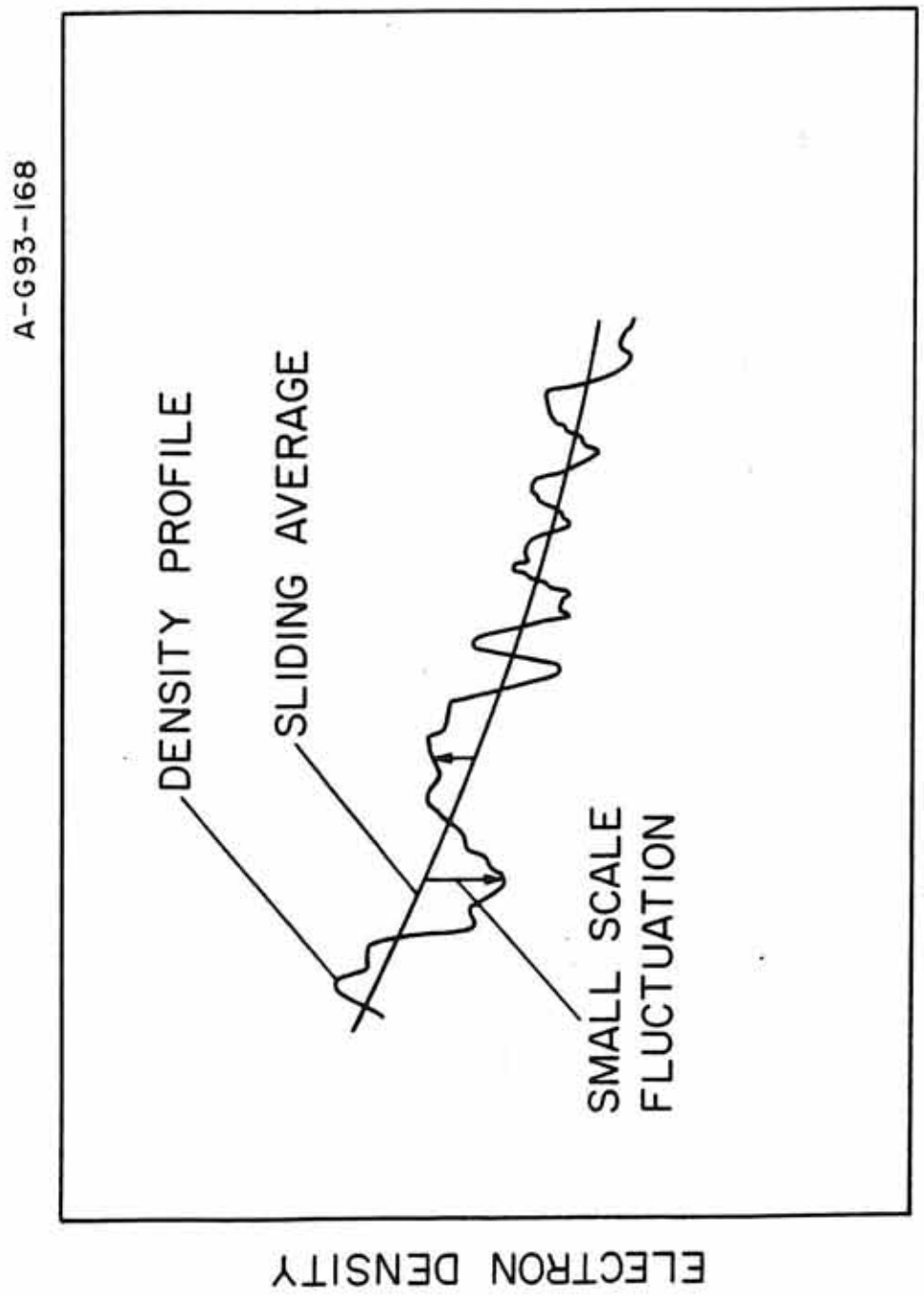
A-G93-168
DENSITY PROFILE
SLIDING AVERAGE
SMALL SCALE
FLUCTUATION
TIME
ELECTRON DENSITY

Figure 6. Log-log plot of the power spectrum for the time series from 02:47:28 UT to 03:15:44 UT, September 15, 1990. The spectral resolution is 0.00082 Hz. A line of slope $-5/3$ is plotted for comparison and a characteristic error bar is shown.

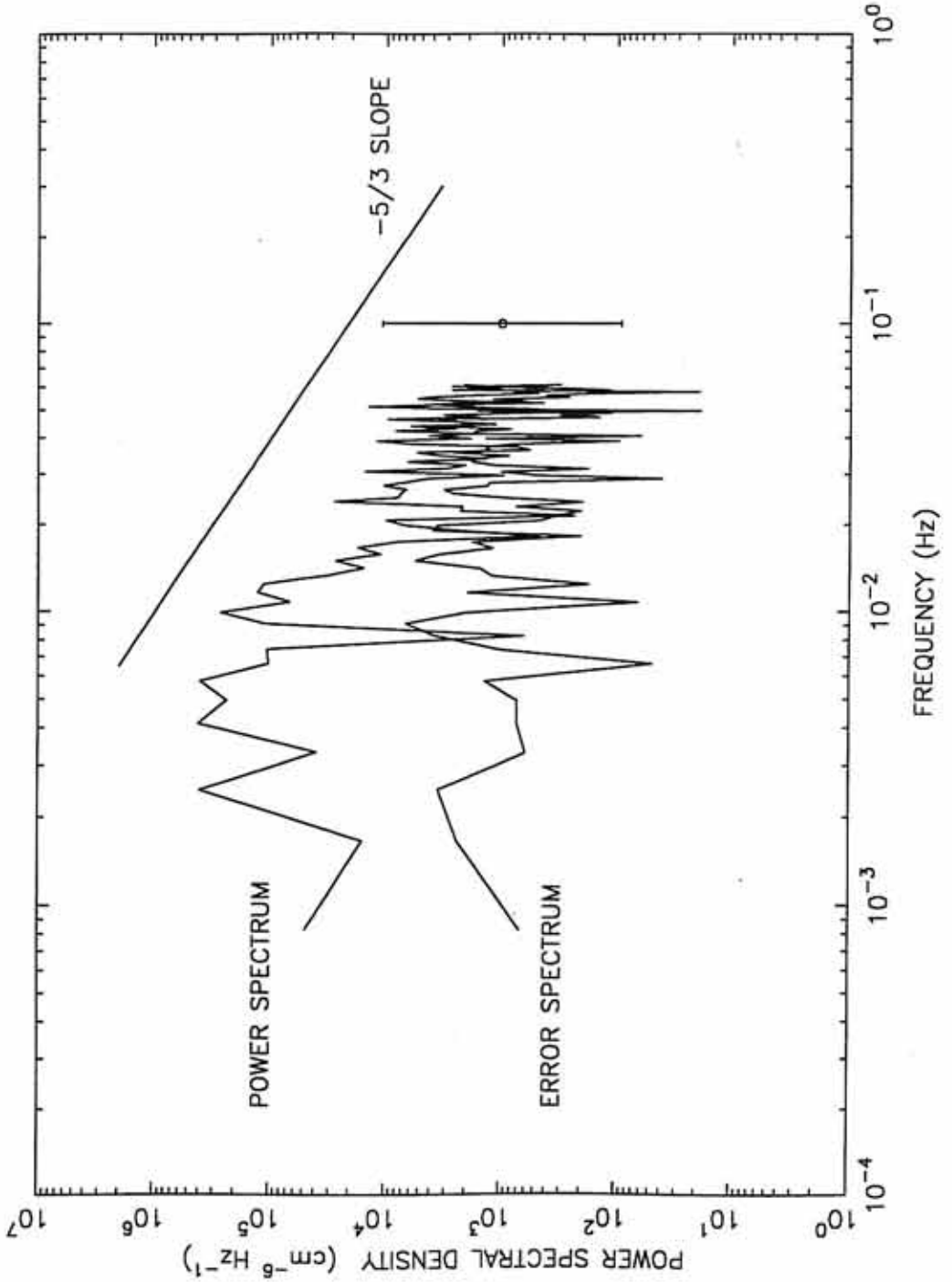
POWER SPECTRUM
ERROR SPECTRUM
-5/3 SLOPE
POWER SPECTRAL DENSITY (cm⁻⁶ Hz⁻¹)
FREQUENCY (Hz)
10⁰
10¹
10²
10³
10⁴
10⁵
10⁶
10⁷
10⁻⁴
10⁻³
10⁻²
10⁻¹
10⁰

Figure 7. Power spectrum for the time series from 02:47:28 UT to 03:15:44 UT, September 15, 1990. The spectrum has been smoothed with a Gaussian filter of width 0.01 Hz.

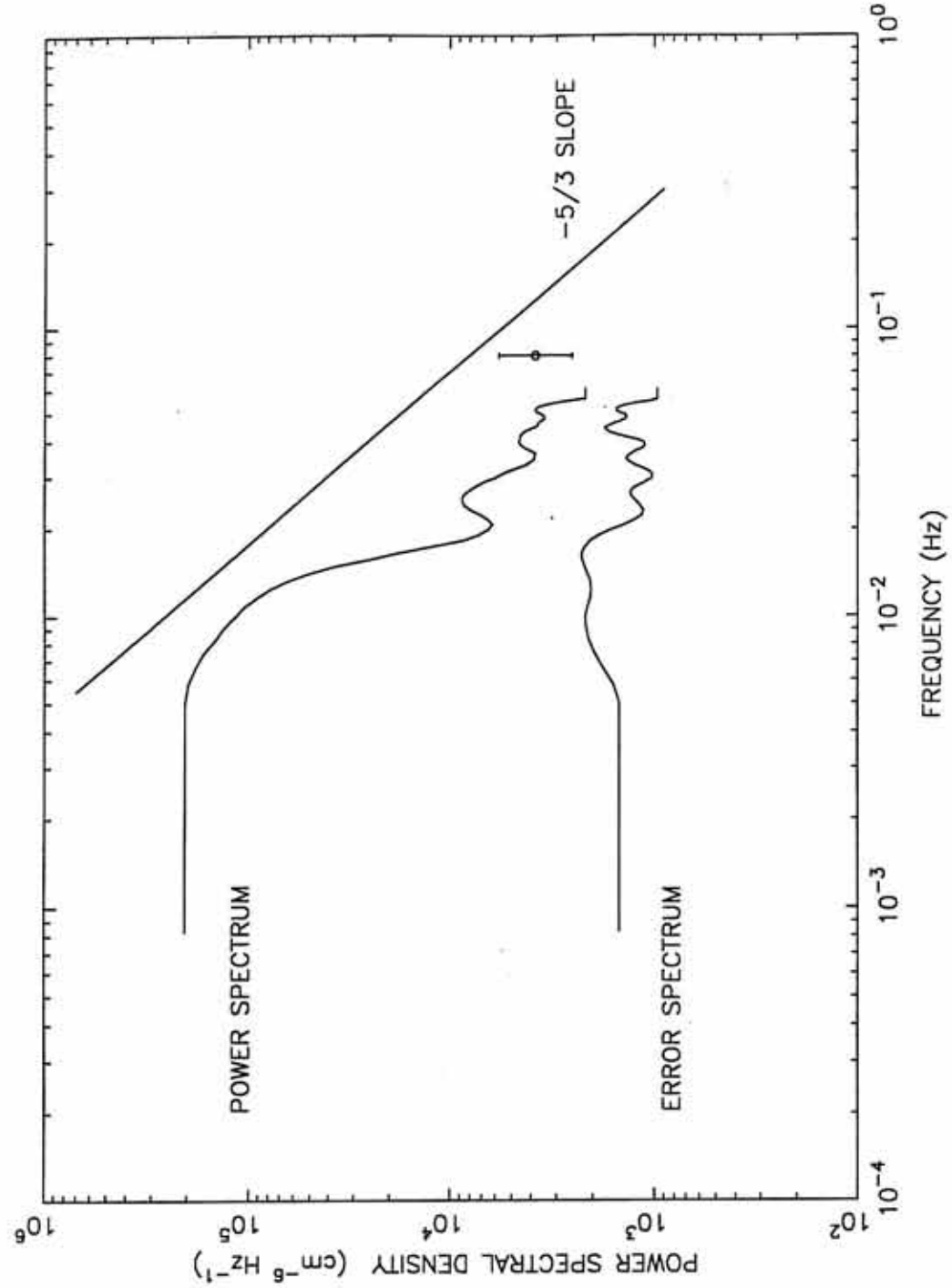
POWER SPECTRUM
ERROR SPECTRUM
-5/3 SLOPE
POWER SPECTRAL DENSITY (cm⁻⁶ Hz⁻¹)
FREQUENCY (Hz)
10⁶
10⁵
10⁴
10³
10²
10⁰
10⁻¹
10⁻²
10⁻³
10⁻⁴

Figure 8. Electron number density profile of the inbound portion of orbit 138. The time series shows data from 21:01:32 UT to 21:28:59 UT, September 20, 1990.

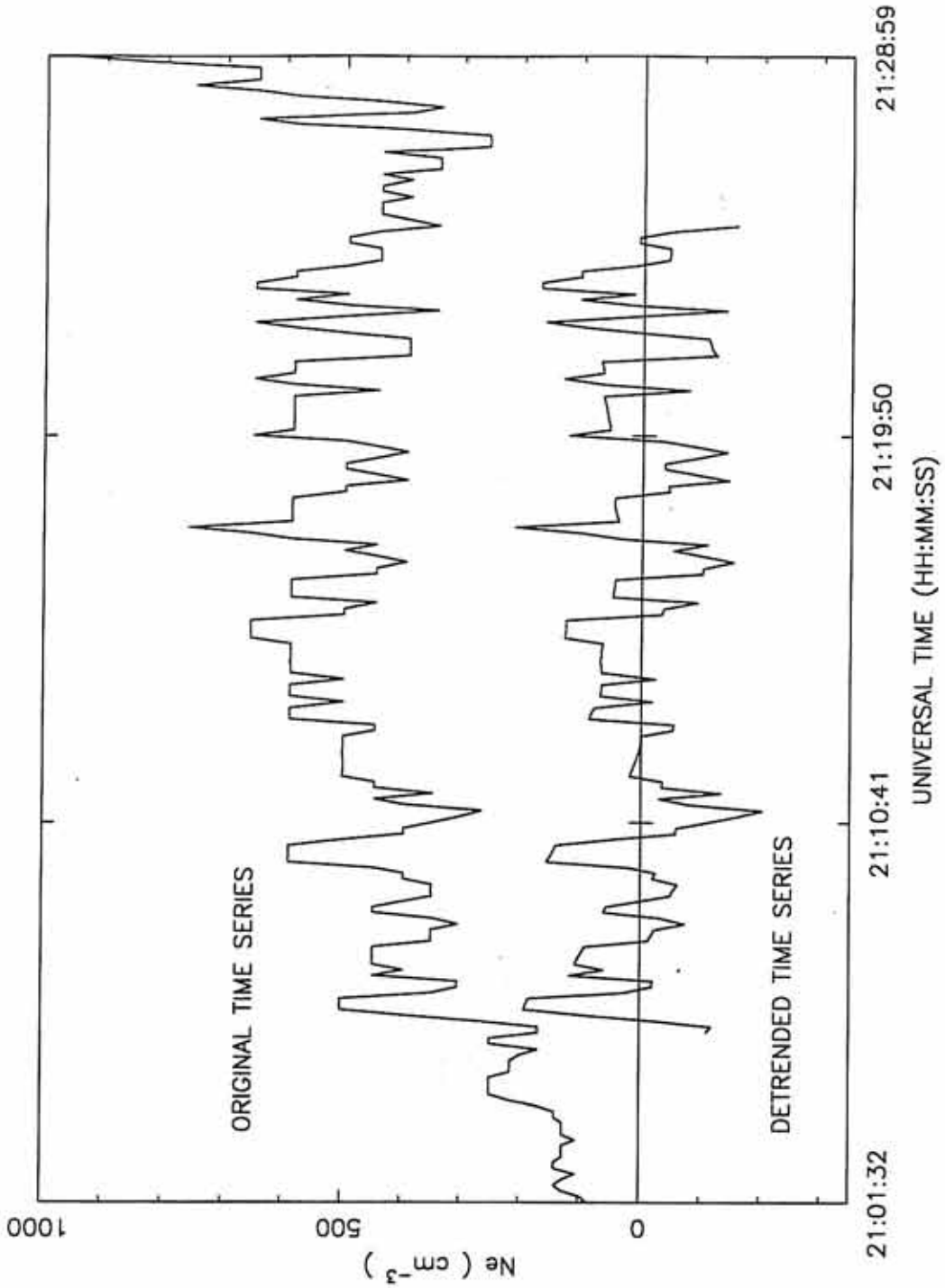
ORIGINAL TIME SERIES
DETRENDED TIME SERIES
Ne (cm⁻³)
1000
500
0
21:01:32
21:10:41
21:19:50
21:28:59
UNIVERSAL TIME (HH:MM:SS)

Figure 9. Log-log plot of the power spectrum for the time series from 21:01:32 UT to 21:28:59 UT, September 20, 1990. The spectral resolution is 0.00086 Hz. A line of slope $-5/3$ is plotted for comparison and a characteristic error bar is shown.

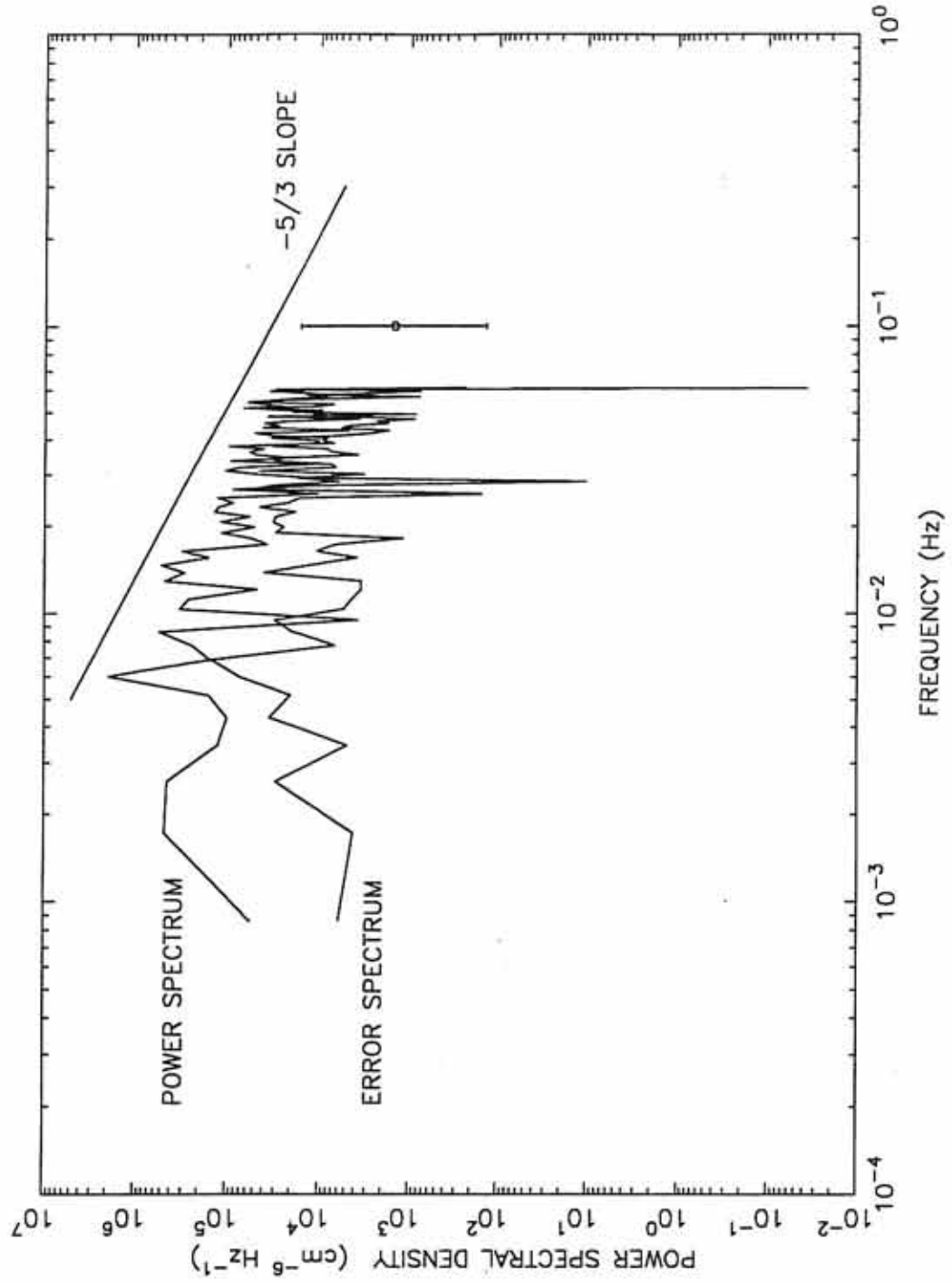
-5/3 SLOPE
POWER SPECTRUM
ERROR SPECTRUM
POWER SPECTRAL DENSITY (cm^{-5} Hz^{-1})
FREQUENCY (Hz)
10^{7}
10^{6}
10^{5}
10^{4}
10^{3}
10^{2}
10^{1}
10^{0}
10^{-1}
10^{-2}
10^{0}
10^{-1}
10^{-2}
10^{-3}
10^{-4}

Figure 10. Smoothed power spectrum for the time series from 21:01:32 UT to 21:28:59 UT, September 20, 1990. The spectral resolution is 0.01 Hz. A line of slope $-5/3$ is plotted for comparison and a characteristic error bar is shown.

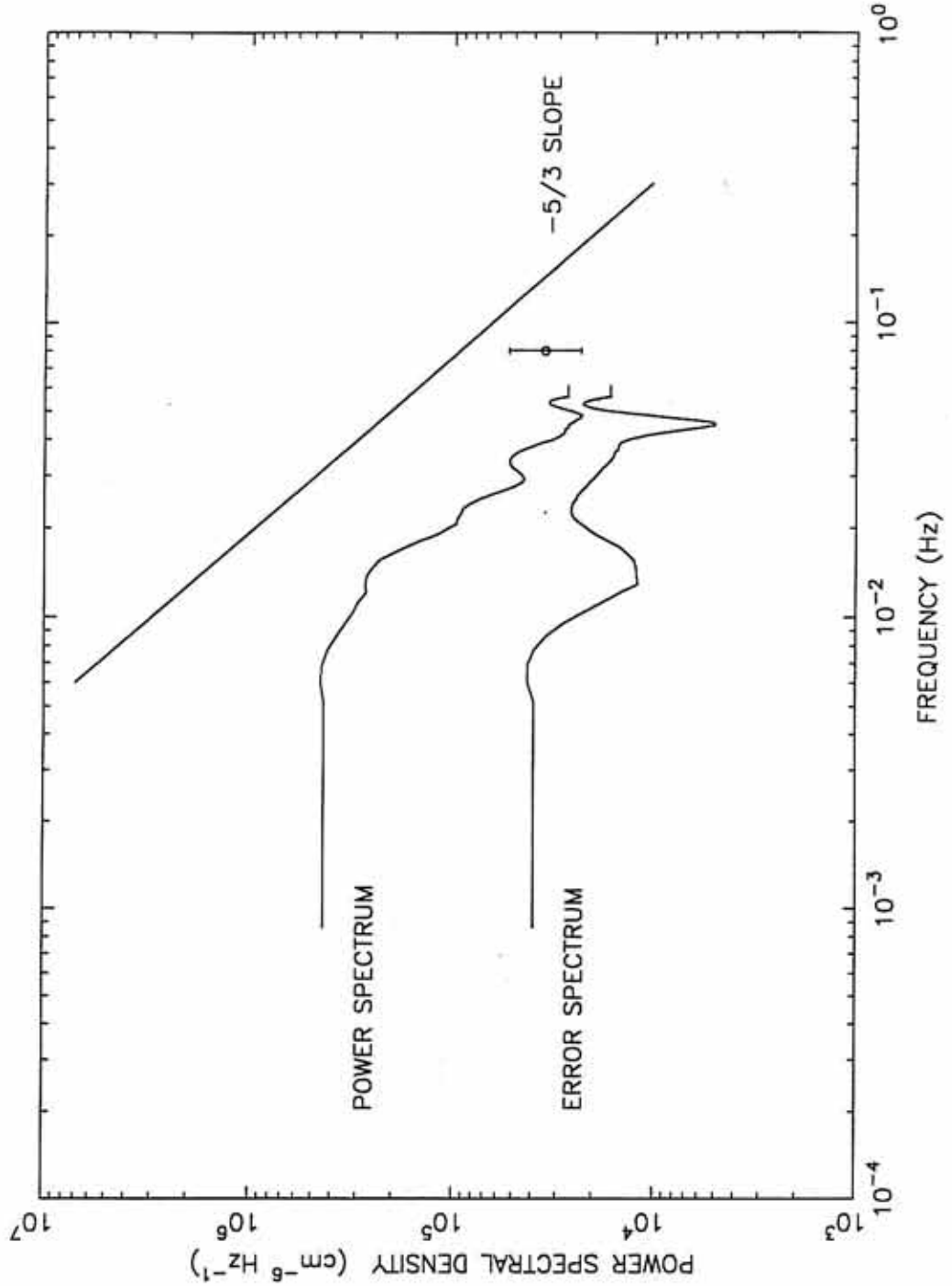
POWER SPECTRUM
ERROR SPECTRUM
-5/3 SLOPE
POWER SPECTRAL DENSITY (cm^{-6} Hz^{-1})
FREQUENCY (Hz)
10^{7}
10^{6}
10^{5}
10^{4}
10^{3}
10^{0}
10^{-1}
10^{-2}
10^{-3}
10^{-4}

Figure 11. Electron number density profile during outbound portion of orbit 99. The time series runs from 14:07:29 UT to 14:35:28 UT, September 4, 1990.

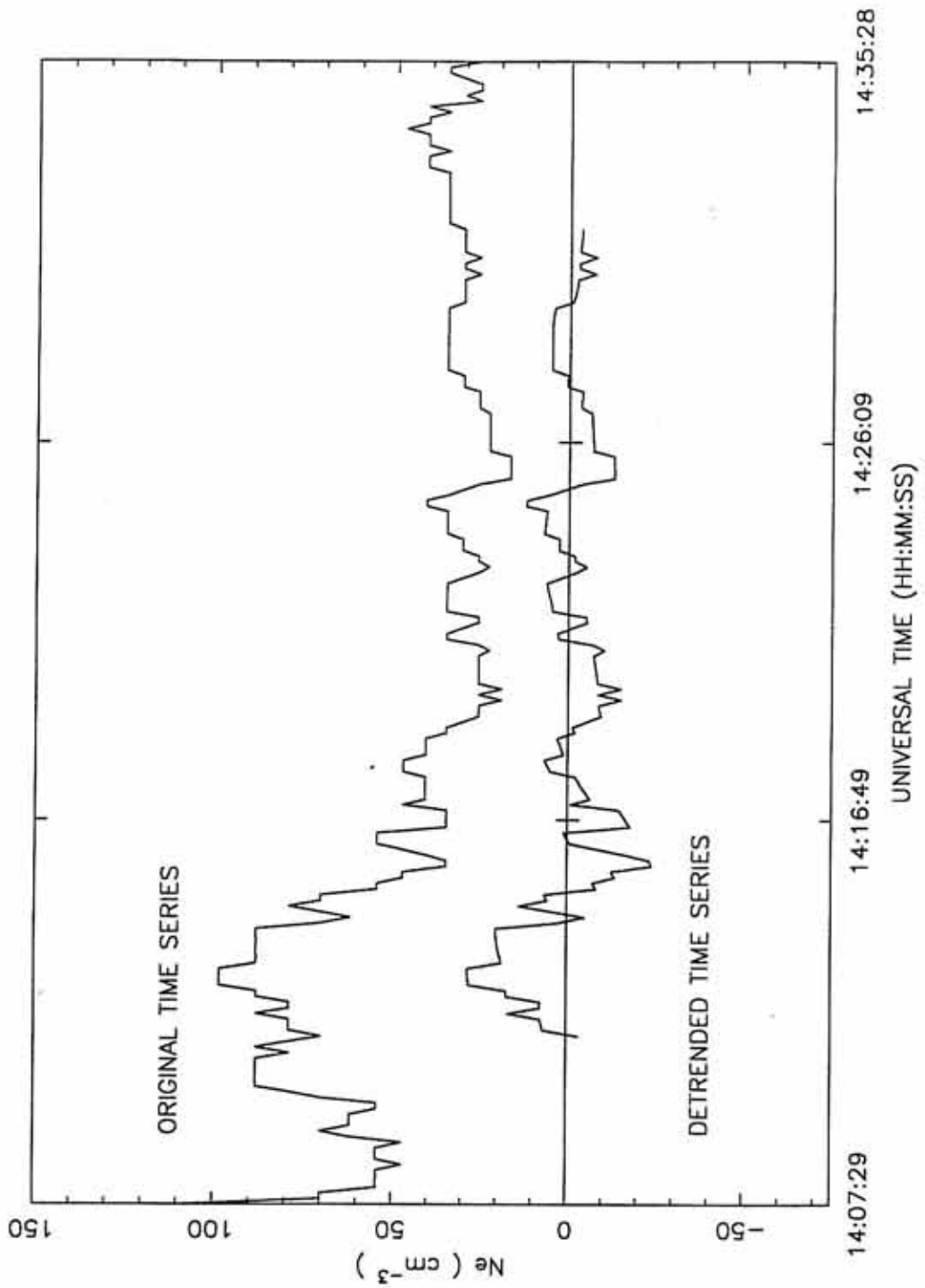
ORIGINAL TIME SERIES
DETRENDED TIME SERIES
Ne (cm^{-3})
150
100
50
0
−50
14:07:29
14:16:49
14:26:09
14:35:28
UNIVERSAL TIME (HH:MM:SS)

Figure 12. Log-log plot of the power spectrum for the time series from 14:07:29 UT to 14:35:28 UT, September 4, 1990. The spectral resolution is 0.00084 Hz. A line of slope $-5/3$ is plotted for comparison and a characteristic error bar is shown.

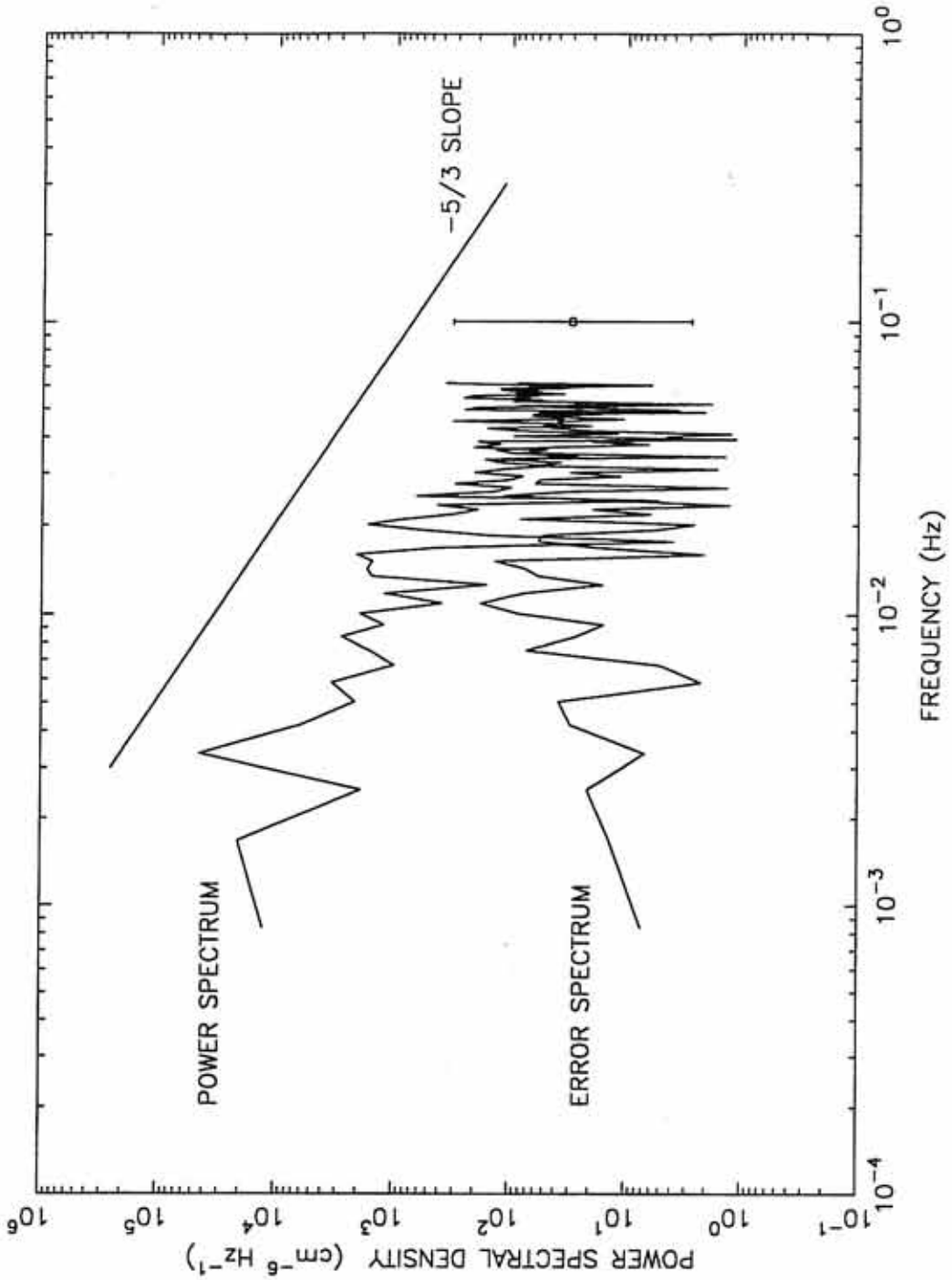
POWER SPECTRUM
ERROR SPECTRUM
-5/3 SLOPE
POWER SPECTRAL DENSITY (cm⁻⁶ Hz⁻¹)
FREQUENCY (Hz)
10⁶
10⁵
10⁴
10³
10²
10¹
10⁰
10⁻¹
10⁻⁴
10⁻³
10⁻²
10⁻¹
10⁰

Figure 13. Smoothed power spectrum for the time series from 14:07:29 UT to 14:35:28 UT, September 4, 1990. The spectral resolution is 0.01 Hz. A line of slope $-5/3$ is plotted for comparison and a characteristic error bar is shown.

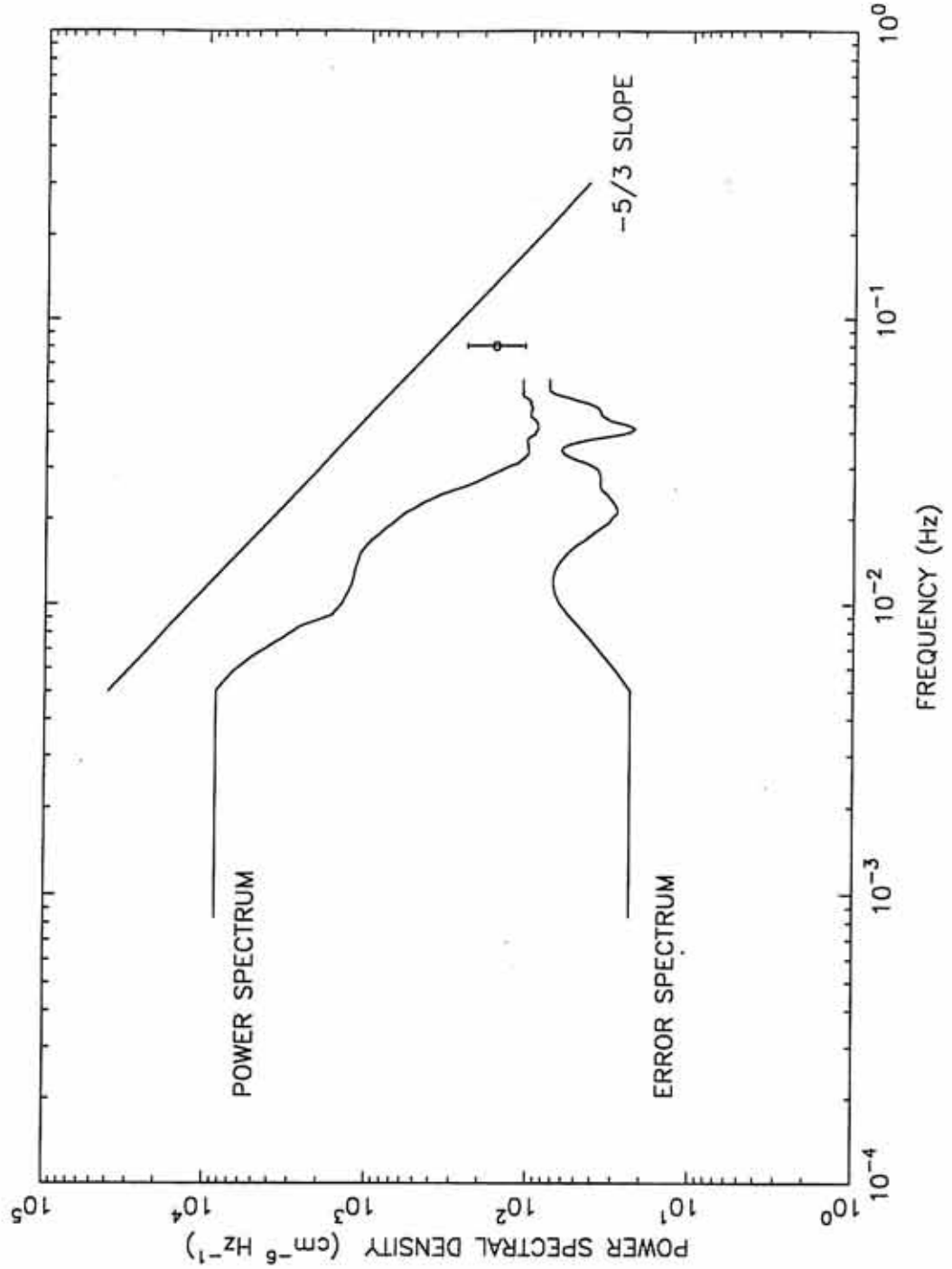
POWER SPECTRAL DENSITY (cm⁻⁵ Hz⁻¹)
10⁵
10⁴
10³
10²
10¹
10⁰
10⁻⁴
10⁻³
10⁻²
10⁻¹
10⁰
FREQUENCY (Hz)
-5/3 SLOPE
POWER SPECTRUM
ERROR SPECTRUM

Figure 14. Electron number density profile at apogee of orbit 251. The time series runs from 01:52:28 UT to 03:41:33 UT, November 6, 1990.

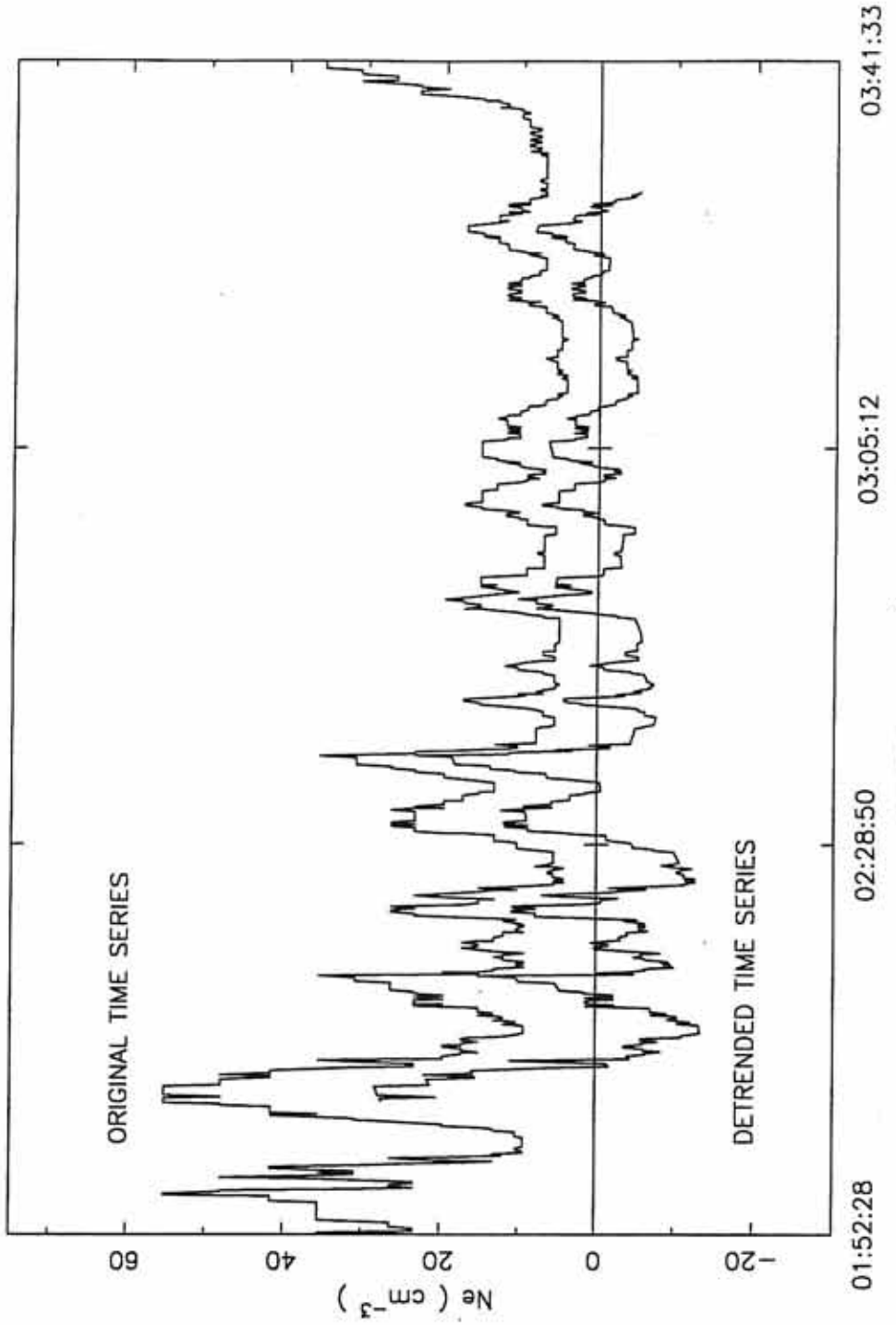
ORIGINAL TIME SERIES
DETRENDED TIME SERIES
Ne (cm^{-3})
60
40
20
0
−20
01:52:28
02:28:50
03:05:12
03:41:33
UNIVERSAL TIME (HH:MM:SS)

Figure 15. Linear plot of the power spectrum for the time series from 01:52:28 UT to 03:41:33 UT, November 6, 1990. The spectral resolution is 0.0001975 Hz. The strong peak occurs at a frequency of about 0.002 Hz.

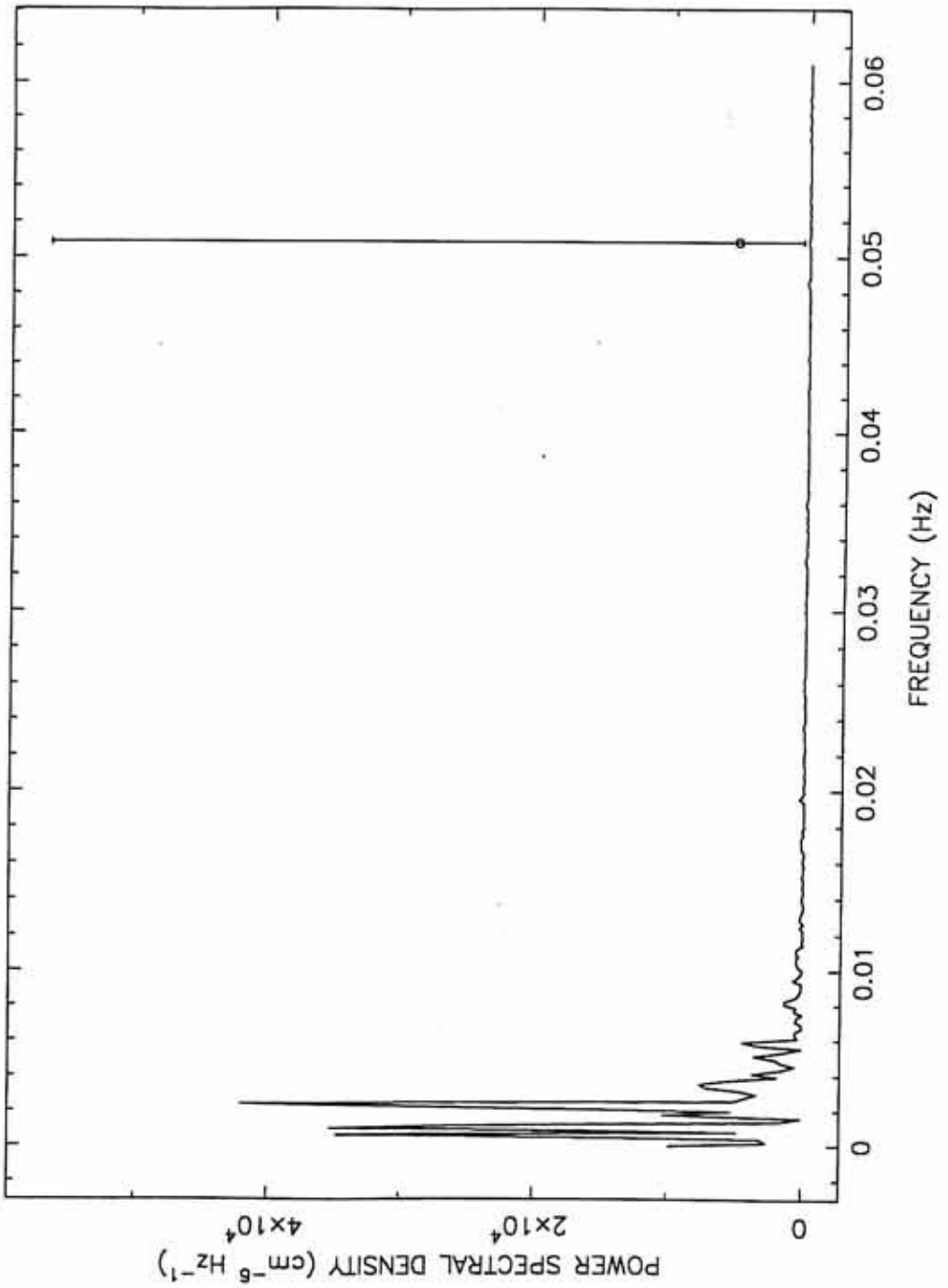
POWER SPECTRAL DENSITY (cm⁻⁶ Hz⁻¹)
0
2×10⁴
4×10⁴
0
0.01
0.02
0.03
0.04
0.05
0.06
FREQUENCY (Hz)

Figure 16. Smoothed power spectrum for the time series from 01:52:28 UT to 03:41:33 UT, November 6, 1990. The spectral resolution is 0.001 Hz. A peak is present at 0.0024 Hz. A representative error bar is shown.

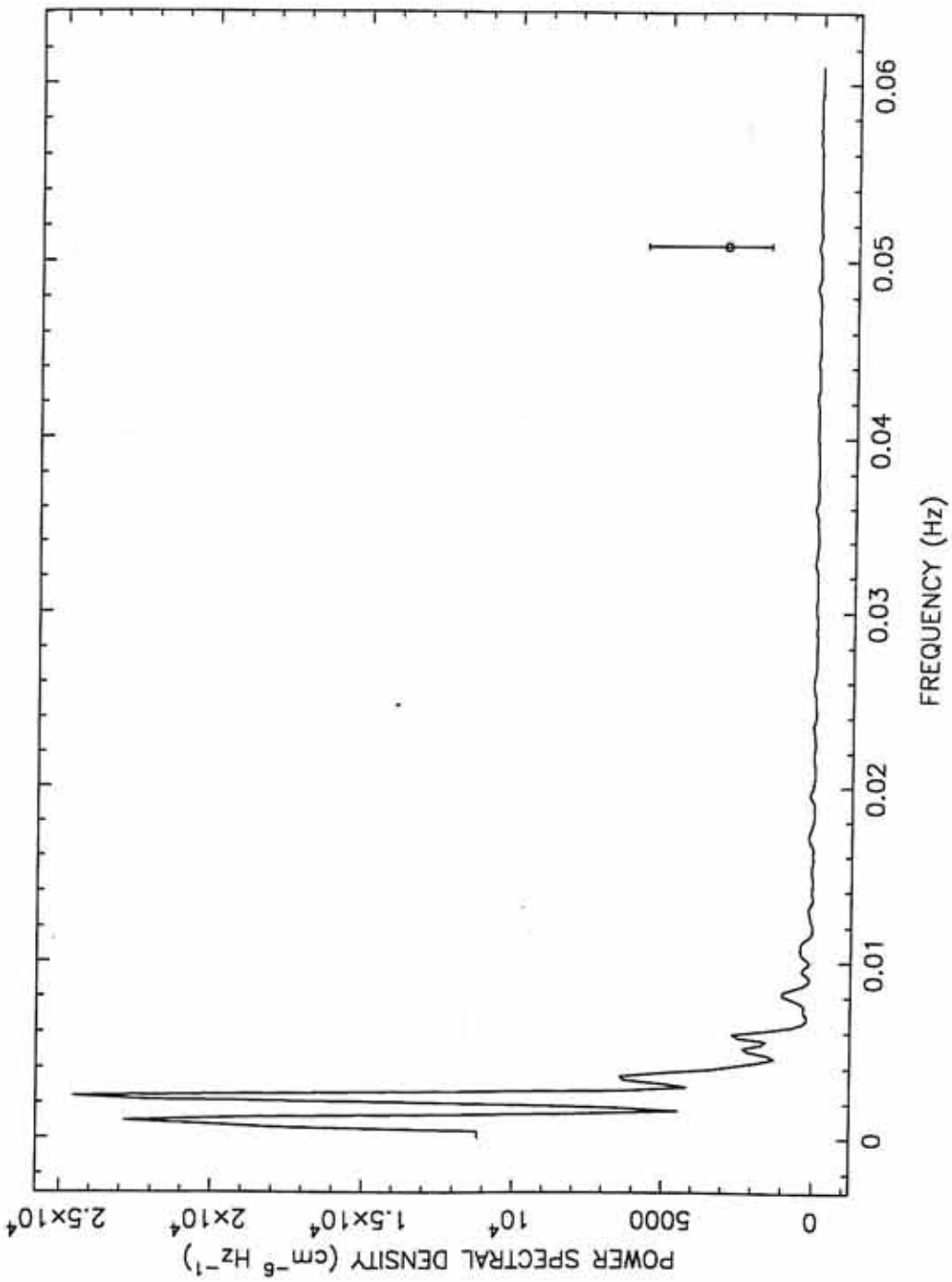
POWER SPECTRAL DENSITY (cm⁻⁶ Hz⁻¹)
0
5000
10⁴
1.5×10⁴
2×10⁴
2.5×10⁴
0
0.01
0.02
0.03
0.04
0.05
0.06
FREQUENCY (Hz)

Figure 17. Scatter plot of the normalized rms density fluctuation amplitude as a function of L-shell. Maximum irregularity amplitudes occur between L = 3 and L = 6.

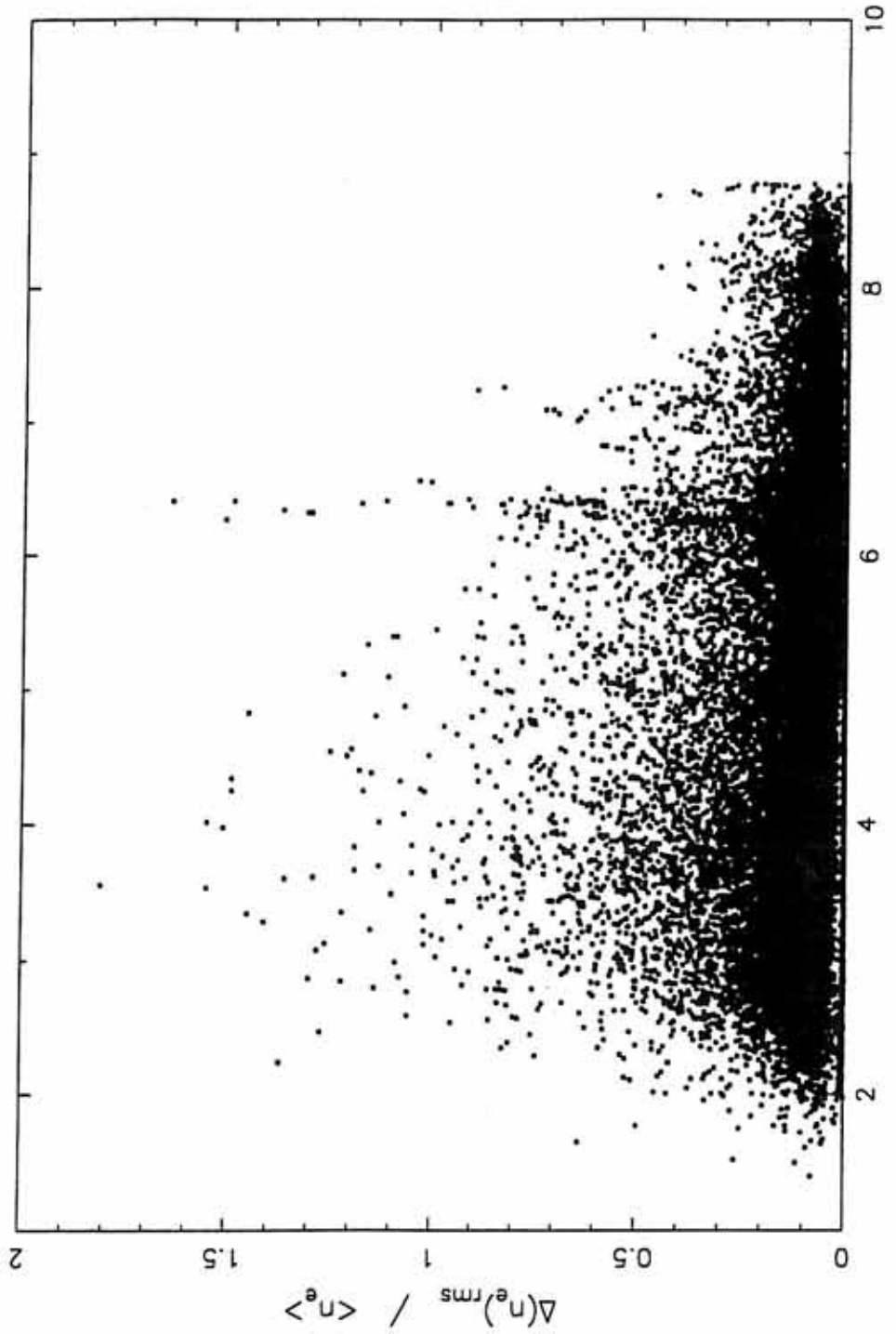
$\Delta(n_e)_{rms}$ / $<n_e>$
0
0.5
1
1.5
2
2
4
6
8
10
L-SHELL

Figure 18. Normalized rms density fluctuation amplitude as a function of L-shell plotted as quartiles. Only the top 25% of the density irregularities are consistently greater than 10% of the average density.

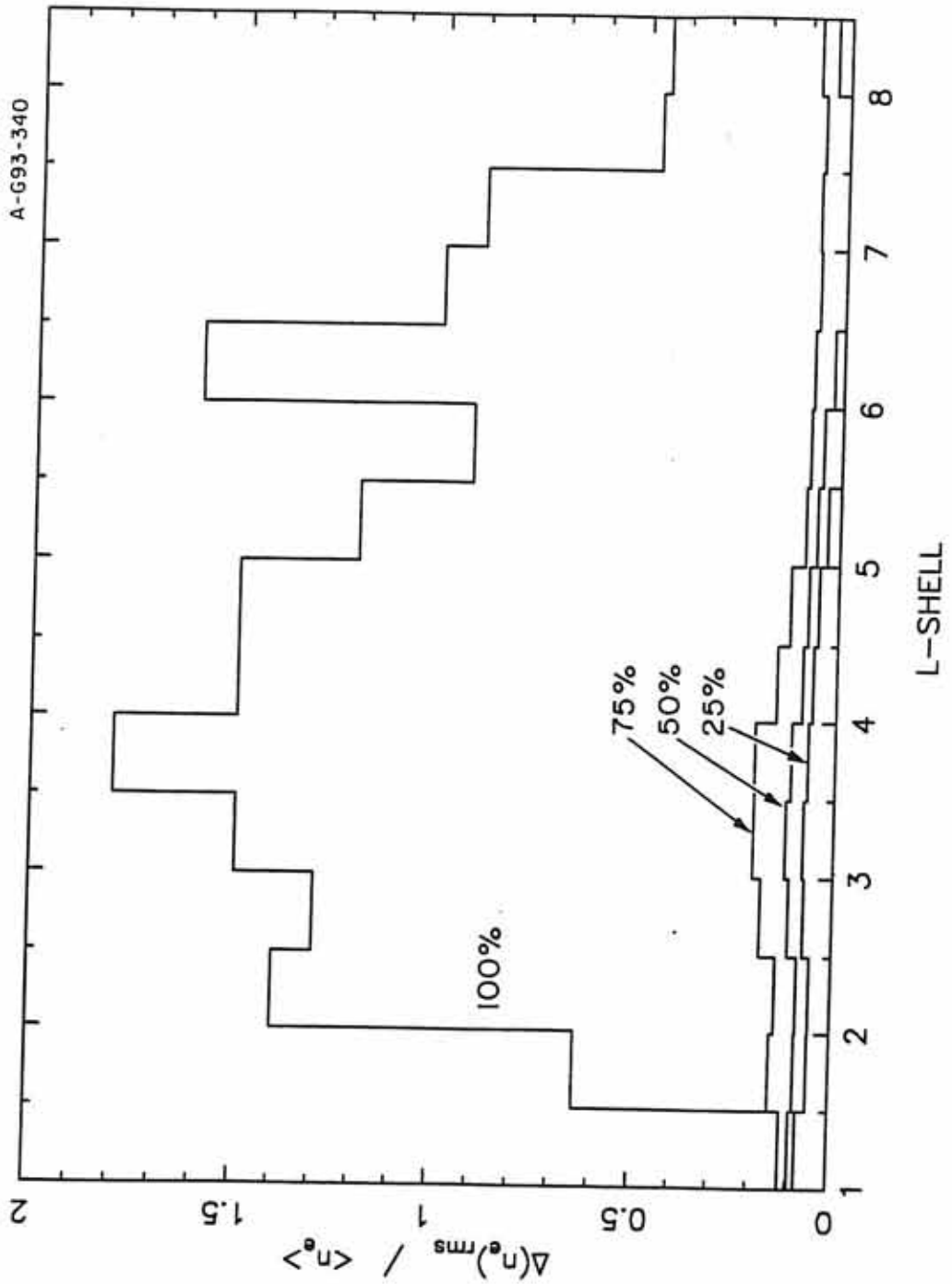
A-693-340
$\Delta(n_e)_{rms} / \langle n_e \rangle$
0
0.5
1
1.5
2
1
2
3
4
5
6
7
8
L-SHELL
100%
75%
50%
25%

Figure 19. Semi-log plot of the normalized rms density irregularity amplitude quartiles as function of L-shell. For L-shell greater than 5.5, 25% to 50% of the fluctuation amplitudes are less than 1% of the local average density.

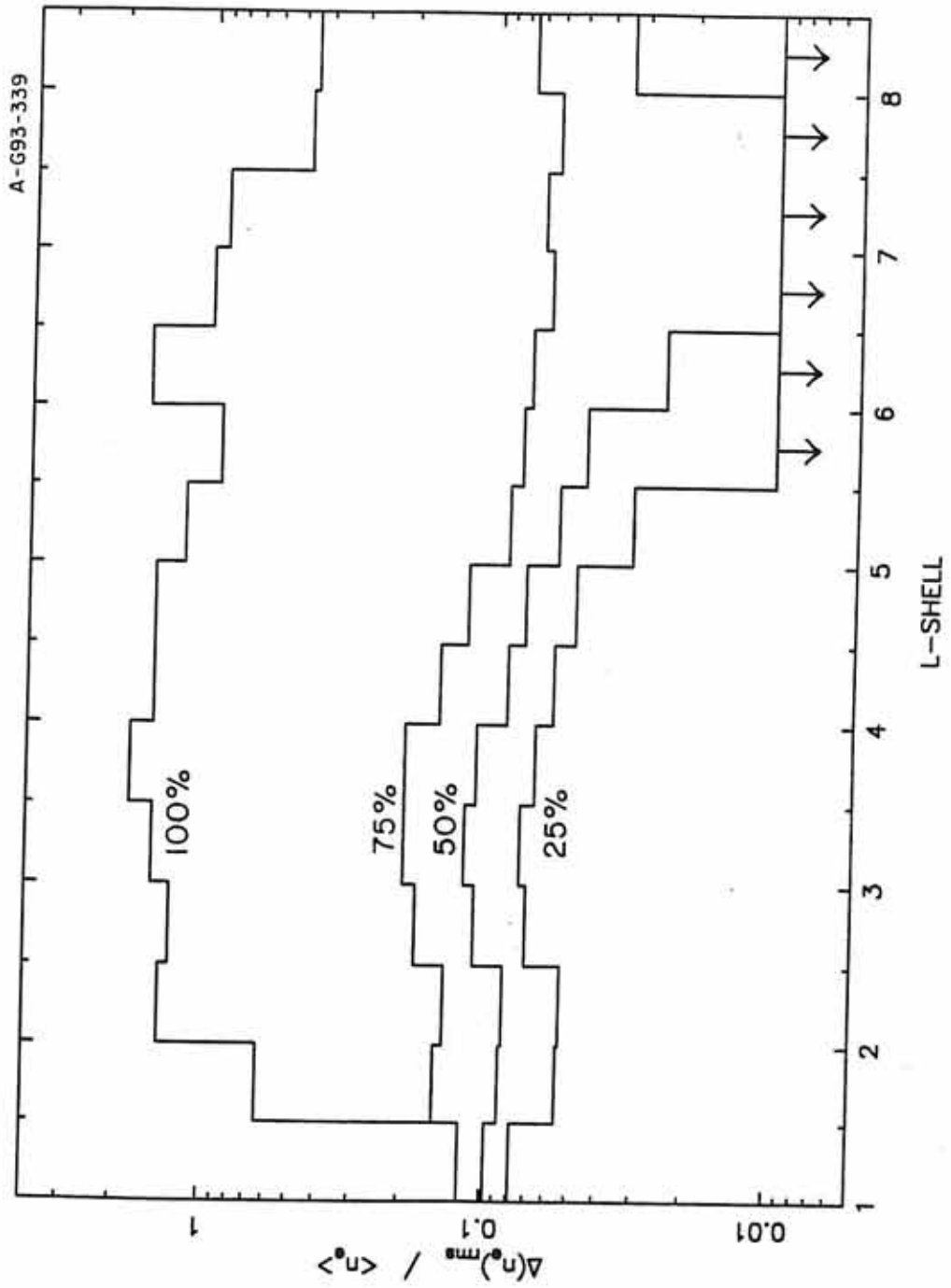
A-G93-339
100%
75%
50%
25%
1
0.1
0.01
1
2
3
4
5
6
7
8
L-SHELL

Figure 20. Scatter plot of normalized rms density irregularity amplitude as a function of L-shell in the 21.00 to 2.99 magnetic local time (MLT) sector.

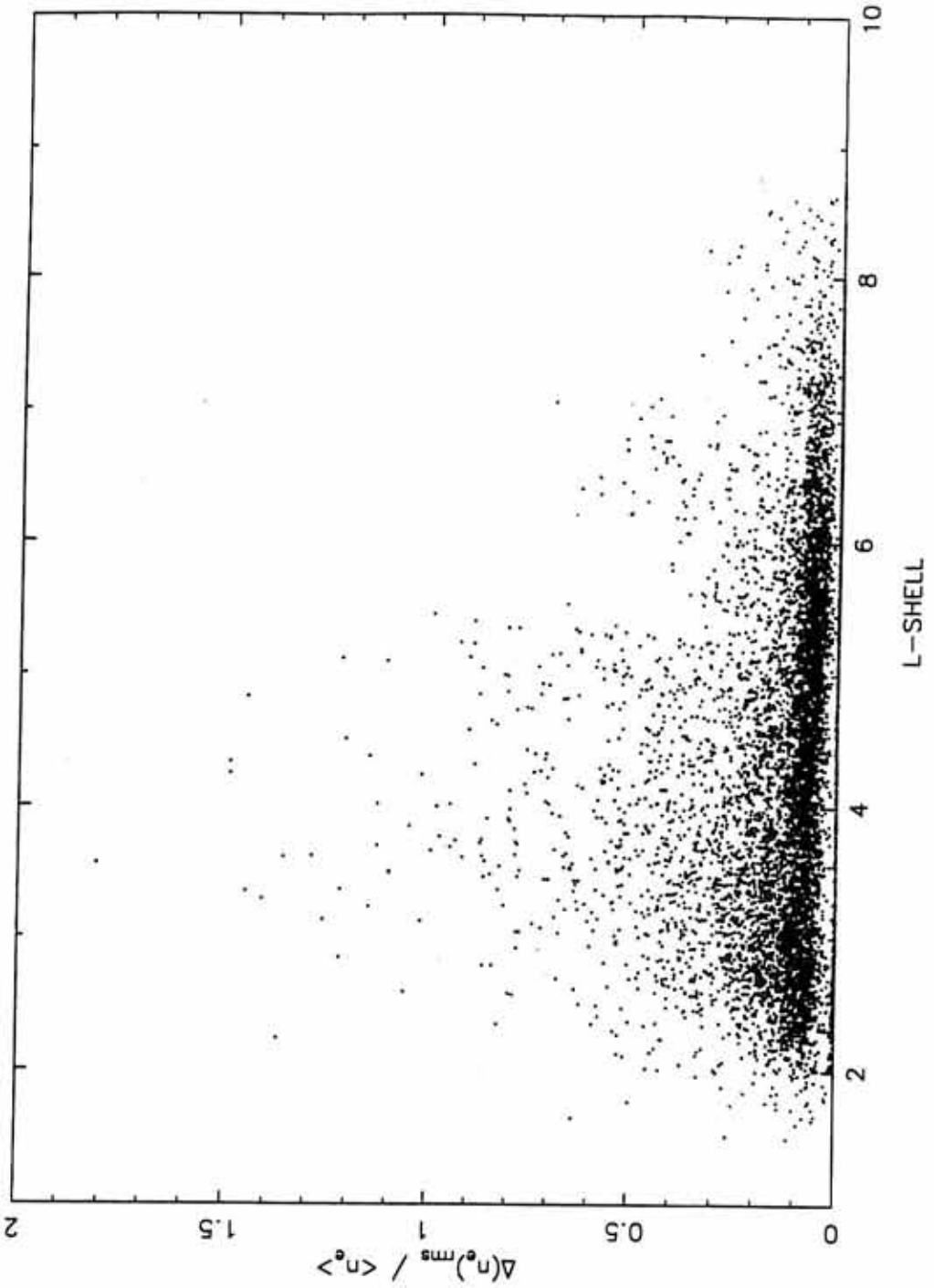
$\Delta(n_e)_{rms}$ / $<n_e>$
0
0.5
1
1.5
2
2
4
6
8
10
L−SHELL

Figure 21. Scatter plot of normalized rms density irregularity amplitude as a function of L-shell in the 3.00 to 8.99 magnetic local time (MLT) sector.

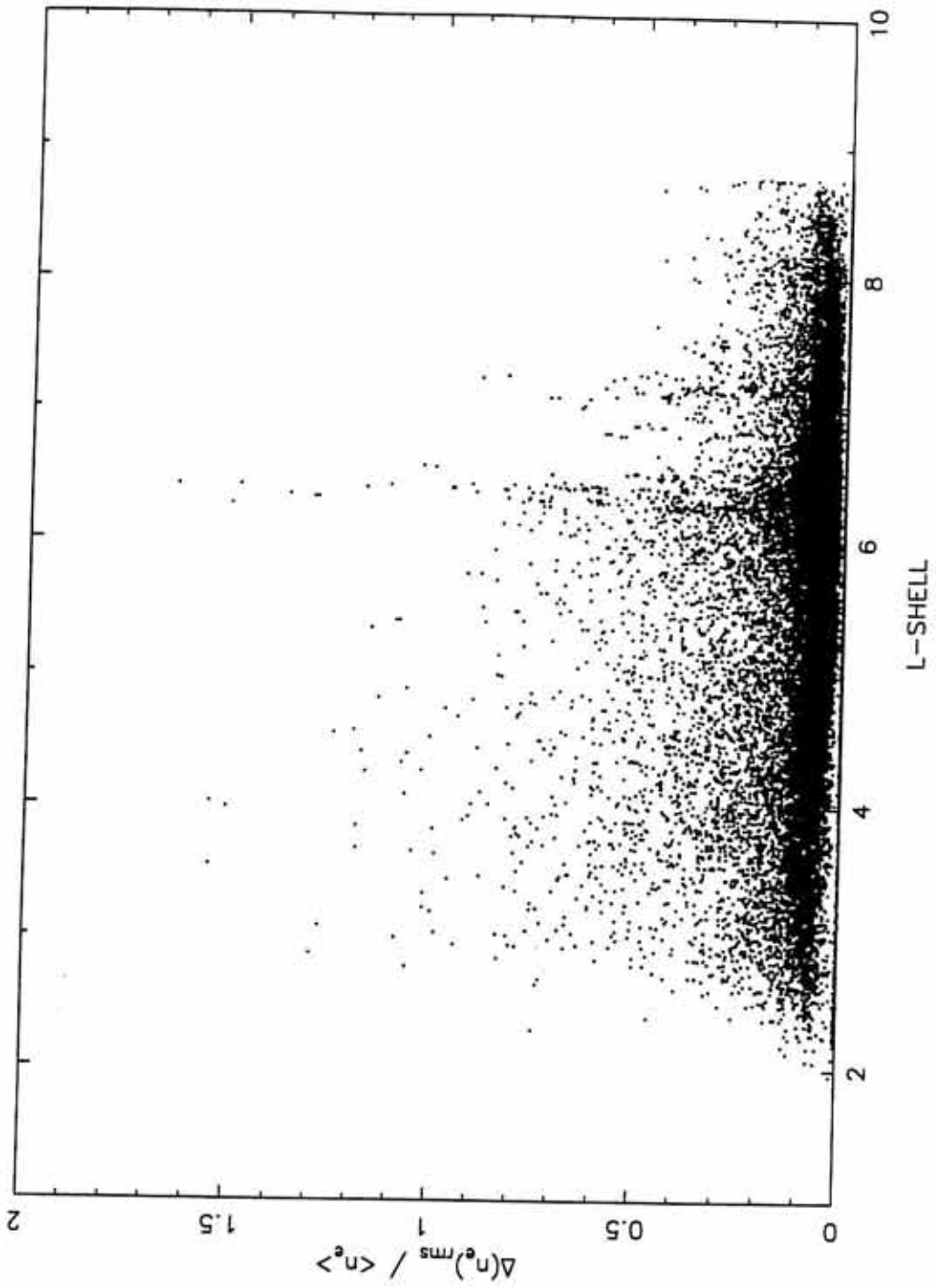
$\Delta(n_e)_{rms}$ / $<n_e>$
0
0.5
1
1.5
2
2
4
6
8
10
L-SHELL

Figure 22. Scatter plot of normalized rms density irregularity amplitude as a function of L-shell in the 9.00 to 14.99 magnetic local time (MLT) sector.

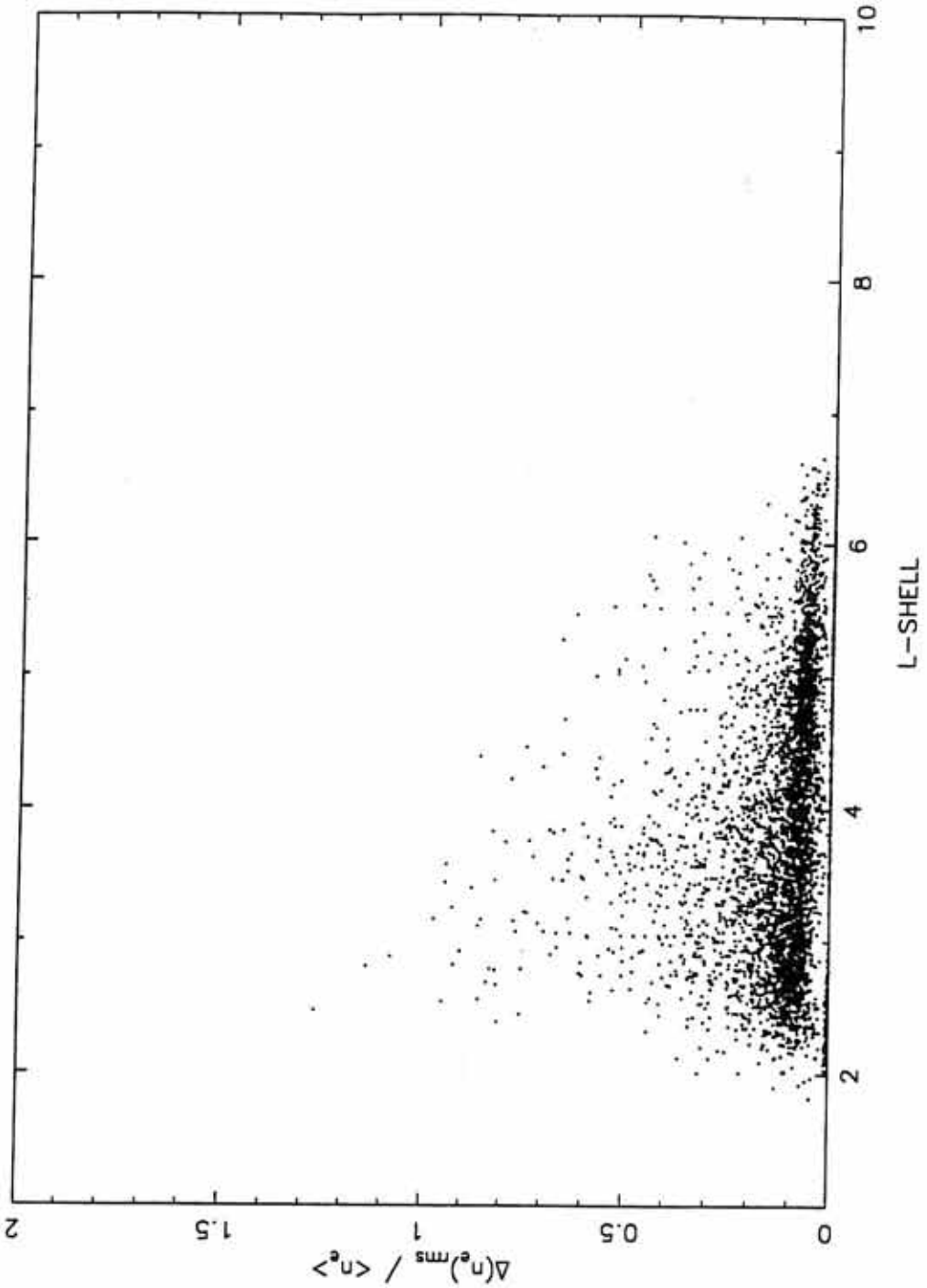
$\Delta(n_e)_{rms}$ / $<n_e>$
0
0.5
1
1.5
2
2
4
6
8
10
L-SHELL

Figure 23. Scatter plot of normalized rms density irregularity amplitude as a function of L-shell in the 15.00 to 20.99 magnetic local time (MLT) sector.

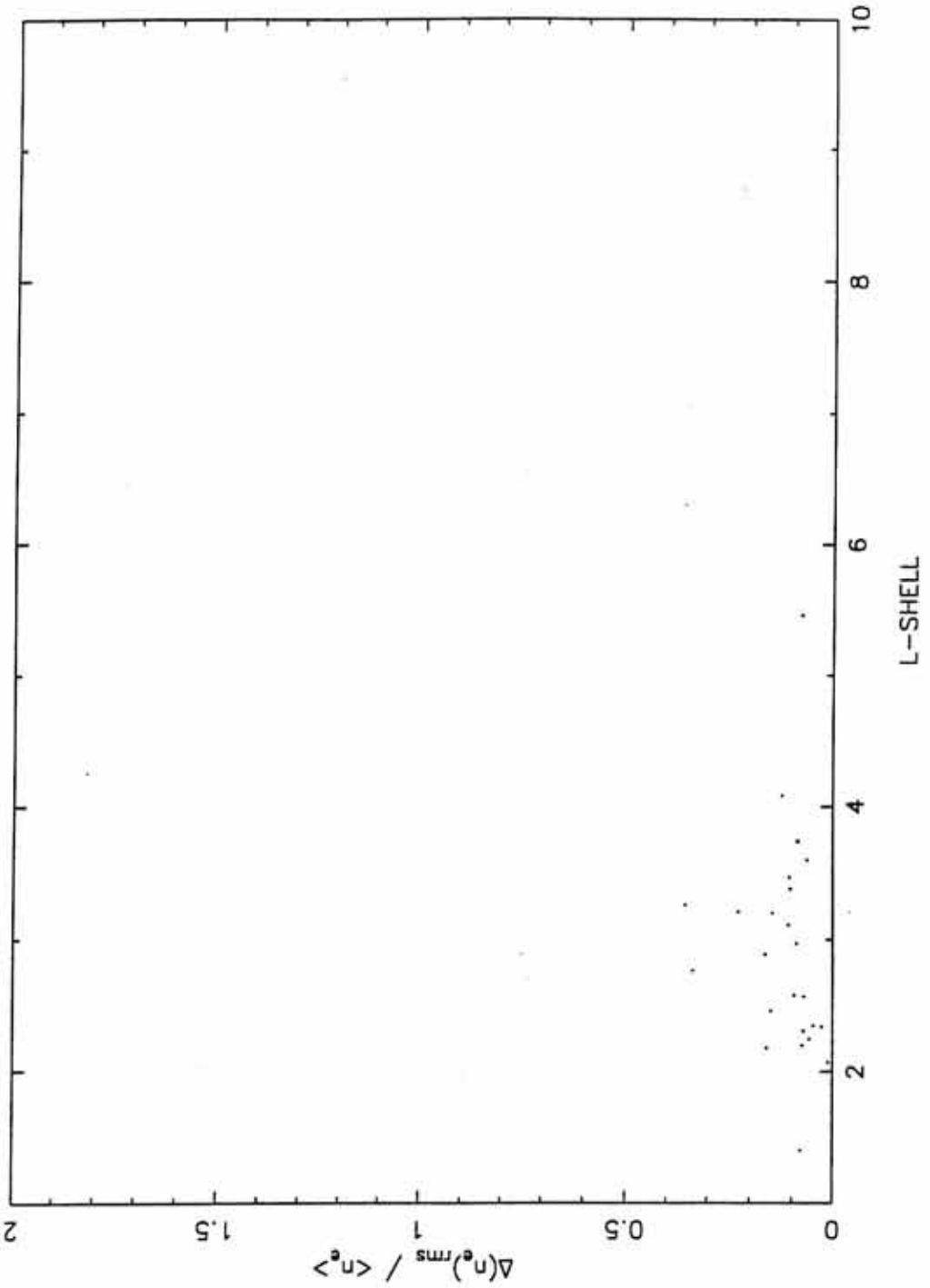
0
0.5
1
1.5
2
$\Delta(n_e)_{rms}$ / $<n_e>$
2
4
6
8
10
L-SHELL

REFERENCES

Anderson, R. R., D. A. Gurnett, and D. L. Odem, CRRES plasma wave experiment, *J. Spac. Rock., 29,* 570, 1992.

Angerami, J. J., and D. L. Carpenter, Whistler studies of the plasmapause in the magnetosphere, 2, Electron density and total tube electron content near the knee in magnetospheric ionization, *J. Geophys. Res., 71*, 711, 1966.

Biskamp, D., and H. Welter, Dynamics of decaying two-dimensional magnetohydrodynamic turbulence, *Phys. Fluids B, 1,* 1964, 1989.

Carpenter, D. L., Whistler studies of the plasmapause in the magnetosphere, 1, Temporal variations in the position of the knee and some evidence on plasma motions near the knee, *J. Geophys. Res., 71,* 693, 1966.

Carpenter, D. L., and C. R. Chappell, Satellite studies of magnetospheric substorms on August 15, 1968, 3. Some features of magnetospheric convection, *J. Geophys. Res., 78,* 3062, 1973.

Chappell, C. R., Detached plasma regions in the magnetosphere, *J. Geophys. Res., 79,* 1861, 1974.

Chappell, C. R., Recent satellite measurements of the morphology and dynamics of the plasmasphere, *Rev. Geophys. Space Phys., 10,* 951, 1972.

Chappell, C. R., K. K. Harris, and G. W. Sharp, The dayside of the plasmasphere, *J. Geophys. Res., 76,* 7632, 1971.

Chappell, C. R., K. K. Harris, and G. W. Sharp, The morphology of the bulge region of the plasmasphere, *J. Geophys. Res., 75,* 3848, 1970.

Chen, A. J., and J. M. Grebowsky, Plasma tail interpretations of pronounced detached plasma regions measured by Ogo 5, *J. Geophys. Res., 79,* 3851, 1974.

Chen, A. J., and R. A. Wolf, Effects on the plasmasphere of a time-varying convection electric field, *Planet. Space Sci., 20,* 483, 1972.

Grebowsky, J. M., and A. J. Chen, Effects on the plasmasphere of irregular electric fields, *Planet. Space Sci., 24,* 689, 1976.

Harris, K. K., and G. W. Sharp, OGO-V ion spectrometer, *Trans. IEEE Geosci., GE-7,* 93, 1969.

Higel, B., Small scale structure of magnetospheric electron density through on-line tracking of plasma resonances, *Space Sci. Rev., 22,* 611, 1978.

Higel, B., and Wu Lei, Electron density and plasmapause characteristics at 6.6 R_E: A statistical study of the GEOS 2 relaxation sounder data, *J. Geophys. Res., 89,* 1583, 1984.

Jacobson, A. R., and W. C. Erickson, Observations of electron-density irregularities in the plasmasphere using the VLA radio-interferometer, submitted to *Annales Geophysicae*, 1992.

Maynard, N. C., and D. P. Cauffman, Double floating probe measurements on S^3-A, *J. Geophys. Res., 78,* 4745, 1973.

Park, C. G., and D. L. Carpenter, Whistler evidence of large-scale electron-density irregularities in the plasmasphere, *J. Geophys. Res., 75,* 3825, 1970.

Park, C. G., and R. A. Helliwell, The formation of field-aligned irregularities in the magnetosphere, *Radio Sci., 6,* 299, 1971.

Sentman, D. D., Basic elements of power spectral analysis, U. of Iowa Research Report 74-5, University of Iowa, Iowa City, Iowa, January 1974.

Shaw, R. R., and D. A. Gurnett, Electrostatic noise bands associated with the electron gyrofrequency and plasma frequency in the outer magnetosphere, *J. Geophys. Res., 80,* 4259, 1975.

Spangler, S., S. Fuselier, A. Fey, and G. Anderson, An observational study of MHD wave-induced density fluctuations upstream of the Earth's bowshock, *J. Geophys. Res., 93,* 845, 1988.